ENERGY PERFORMANCE ANALYSIS AND MATERIALS CHARACTERIZATION OF AEROGEL INSULATION BLANKETS

A Thesis Submitted to
the Graduate School of Engineering and Sciences of
İzmir Institute of Technology
in Partial Fulfillment of the Requirements for the Degree of

MASTER OF SCIENCE

in Energy Engineering

by
Selena ALAN

July 2022
İzmir

ACKNOWLEDGEMENTS

ABSTRACT

ENERGY PERFORMANCE ANALYSIS AND MATERIALS CHARACTERIZATION OF AEROGEL INSULATION BLANKETS

İzmir Geothermal Energy Inc. is a geothermal district heating company in İzmir-Turkey that circulates hot water throughout the district via a 450 km of piping system and with the help of valves, pipes, and heat exchangers. As the distance traveled by the hot water is excessively long, heat losses are common. Rock wool is used as thermal insulation material, but the performance degraded over time because of water leakage. Instead of rock wool, aerogel insulation blanket use is evaluated in this study.

Rock wool and three different aerogel insulation blankets are comparatively studied to assess their structures and thermal performances in two ways: the first is the characterization of materials by various physical and chemical analysis methods in the IZTECH-Integrated Research Center. The second way is to assemble a test setup on-site and make thermal measurements on the test setup for each aerogel insulation material, rock wool, and bare pipe. Heat loss calculations were conducted by EES software. The results are compared based on each characterization and thermal performance calculation.

The thermal conductivity values of the insulation materials were calculated. Non-wetting properties were also checked to understand their hygrothermal properties. Compared with bare pipe, with the 10 mm thickness, rock wool decreases heat loss by 48-52%, and with the 10 mm thickness, the aerogel insulation blankets reduce heat loss by 57-61%. Finally, while aerogel insulation blankets have a better performance, they are more expensive than rock wool.

Keywords: *Aerogel, Insulation, Geothermal Energy, Energy Efficiency*

ÖZET

AEROJEL YALITIM BATTANİYELERİNİN ENERJİ PERFORMANS ANALİZİ VE MALZEME KARAKTERİZASYONU

İzmir Jeotermal Enerji A.Ş., İzmir-Türkiye'de sıcak suyu 450 km'lik boru sistemi ile vana, boru ve ısı eşanjörleri yardımıyla ilçe genelinde dolaştıran bir jeotermal bölgesel ısıtma şirketidir. Sıcak suyun kat ettiği mesafe aşırı uzun olduğu için ısı kayıpları yaygındır. Isı yalıtım malzemesi olarak taş yünü kullanılmaktadır, ancak su sızıntıları nedeniyle performansı zamanla düşmektedir. Bu çalışmada taş yünü yerine aerojel yalıtım levha kullanımı değerlendirilmiştir.

Taş yünü ve üç farklı aerojel yalıtım battaniyesi, yapılarını ve termal performanslarını iki şekilde değerlendirmek için karşılaştırmalı olarak incelenmiştir: ilki, malzemelerin İYTE-Tümleşik Araştırma Merkezi'nde çeşitli fiziksel ve kimyasal analiz yöntemleriyle karakterizasyonudur. İkinci yöntem, her aerojel yalıtım malzemesi, taş yünü ve çıplak boru için yerinde bir test düzeneği kurmak ve test düzeneğinde termal ölçümler yapmaktır. Isı kaybı hesaplamaları EES yazılımı ile yapılmıştır. Sonuçlar, her bir karakterizasyon ve termal performans hesaplamasına dayalı olarak karşılaştırılmıştır.

Yalıtım malzemelerinin ısıl iletkenlik değerleri hesaplanmıştır. Higrotermal özelliklerini anlamak için ıslanmama özellikleri de kontrol edilmiştir. Çıplak boru ile karşılaştırıldığında, 10 mm kalınlığındaki taş yünü ısı kaybını %48-52, 10 mm kalınlığındaki aerojel yalıtım battaniyeleri ise ısı kaybını %57-61 oranında azaltır. Son olarak, aerojel yalıtım battaniyeleri daha iyi performans gösterirken taş yününden daha pahalıdır.

Anahtar Kelimeler: *Aerojel, Yalıtım, Jeotermal Enerji, Enerji Verimliliği*

TABLE OF CONTENTS

LIST OF FIGURES

LIST OF TABLES

LIST OF SYMBOLS

A	Area	m^2
C_p	Specific heat capacity	j/gK
D	Diameter	m
f	Friction factor	-
g	Gravitational acceleration	m/s^2
h	Convective heat transfer coefficient	W/m^2K
k	Conductive heat transfer coefficient	W/mK
L	Length	m
m	Mass	kg
Nu	Nusselt number	-
Pr	Prandl number	-
Q, q	The heat loss	W
r	Radius	m
Ra	Rayleigh number	-
Re	Reynolds number	-
R	Thermal resistance	m^2K/W
T	Temperature	K
U	Overall heat transfer coefficient	W/m^2K
V	Volume	m^3
v	Velocity	m/s

Greek Letters

α	Thermal diffusivity	m^2/s
β	Coefficient of thermal expansion of the fluid	1/K
Δ	Difference	-
ε	Emissivity	-
σ	Stefan Boltzmann constant	W/m^2K^4
ϑ	Kinematic viscosity	m^2/s
ρ	Density	kg/m^3
μ	Viscosity	kg/ms

Subscripts

a   Annual

conv   Convection

f   Mean value (air film)

i   Inside, internal

ins   Insulation

o   Outside, external

os   Outer surface of pipe

rad   Radiation

s   Surface

t   Total

CHAPTER 1

INTRODUCTION

Population growth, industrialization, growth in investments, and rising living standards in the World and our country necessitate technological and scientific studies in the field of energy. With the increase in the number of people globally, excessive energy consumption causes a decrease in living standards. Therefore, energy has become a global problem today. The most important way to solve this problem is to use energy more efficiently or turn to alternative energy sources.

About one-third of Turkey's energy consumption occurs in the housing sector. 85% of energy consumption in residential buildings is spent for heating and domestic hot water production [1]. The residential buildings and especially industrial plants contain complex and expensive pipe structures. Piping systems are used in many situations, including water supply, fire protection, and district cooling-heating applications. The type and characteristics of heating systems are essential in terms of energy efficiency and economy. Among the heating systems, district heating gains importance for efficiently using energy resources and assembling the heat needed regularly, adequately, and generally cheaper than other methods. Heating systems are grouped into three main groups [1].

• Local heating: Heat is produced and consumed in the space to be heated (heating with a fireplace, stove, or electric heaters).

• Central heating: The heat produced in a center is sent to the heaters in the volume to be heated using a carrier fluid (such as heating one or more volumes or a building from a boiler room).

• District heating: It is the way in which the buildings in a region are heated by the heat produced in a center (such as university campuses), all of a small city, or a part of a large city. Traditional thermal insulation materials used in the hotlines as district heating pipelines are; glass wool, rock wool, glass foam, and ceramic wool. The district heating system decreases heat losses through the district and buildings.

In Turkey, national regulations are initiated to reduce energy consumption to minimum values. In May 2008, TS 825 "Thermal Insulation Rules for buildings" [2] standard was issued. TS 825 include two critical clauses about standard pipe insulation;

- Plumbing pipes must not be located on external walls. This precaution is important in terms of making full use of the fuel and preventing the installation pipes from freezing.
- The main distribution (plumbing) pipes that transmit the hot fluid in the buildings heated by the central system should be properly insulated by calculating the economic insulation thickness.

Following TS 825, the "Energy Performance of Buildings Directive" [3] was entered into force on 5 December 2008. About hot water-carrying pipes;

- Sanitary hot water generators and storage units are insulated against heat losses from their surfaces through convection and radiation, moisture, condensation, and corrosion, considering the economic conditions. A minimum of 80 mm thick insulation material with a maximum of 0.040 W/mK thermal conductivity coefficients.
- Pre-insulated pipes carrying hot or cold fluids buried underground should be selected considering the economic conditions and resistance to heat losses/gains, humidity, condensation, and corrosion. Depending on the system requirements, suitable equipment is used to detect losses and leaks in steel pipe installations.

Therefore, the insulation of the used pipes and equipment gains importance to reduce heat losses from the heating systems. Appropriate insulation in piping systems becomes very important in energy saving. In selecting the insulation material, the average outdoor temperature of the region, the thermal conductivity of the insulation material, the water absorption property of the material, and its cost are the most important parameters. As the thickness of the insulation material increases, the energy consumption for heating will decrease. On the other hand, determining the optimum insulation thickness gains importance as the cost increases with increasing insulation thickness.

In geothermal heating systems, all machinery and equipment required for geothermal energy use can be produced domestically. The advantages of geothermal energy usage; it is a national energy source, cheap, has no risk, and is safe; there is an

almost infinite source of energy underground; it provides year-round, low-cost heating and cooling using district heat energy technology.

Installing a district heating system requires significant upfront capital investment. Large diameter insulated pipes are necessary for the hot water network; heat losses may increase in large systems with this diameter and piping length. The heat produced in the summer can be wasted.

In geothermal district heating systems, geothermal fluid is transported at moderate-high temperatures (90-150°C). In the piping system installed underground and/or above ground, water leaks may occur over time, and therefore corrosion may occur in the pipes.

Insulation materials are produced according to the temperature of the fluid passing through the pipes. In cold lines (T<+6°C), polyethylene, rubber foam, glass wool, rock wool, EPS (Expanded Polystyrene), XPS (Extruded Polystyrene), and polyurethane can be used. In warm lines (+6<T<100°C), polyethylene, rubber foam, glass wool, rock wool, glass foam, and polyurethane can be used. On hotlines (T>100°C), rubber foam, glass wool, rock wool, glass foam, ceramic wool, and calcium silicate can be used [4]. For high performance insulation, aerogels and VIP (vacuum insulation panels) can be selected. Some properties of some of the insulation materials are given in Table 1 [4].

Table 1. Some properties of thermal insulation materials [4].

Insulation material	Max. operating temperature ([°C)	Thermal conductivity (k) at 10°C (W/mK)	Density (kg/m^3)
Glass wool	250	0.030-0.050	10-120
Rock wool	750	0.035-0.050	20-200
EPS	75/80	0.030-0.040	15-30
XPS	75/80	0.030-0.040	25-50
Polyethylene foam	95	0.035-0.050	30-40
Rubber foam	110	0.030-0.050	45-65

Due to the non-wetting properties and low thermal conductivity, aerogel blankets can be applied as an insulation material in order to reduce rapid corrosion and loss of heat. Energy can be saved with the insulation on piping, valve, and heat exchanger systems. With saved energy, it can provide extra energy to more residences, and if it is necessary, production wells can be rested.

The primary source of district heating systems in Turkey is geothermal. There are facilities in 26 different regions, and improvement works are also continuing. They are in Afyon, Ağrı, Ankara, Balıkesir, Bursa, Denizli, İzmir, Kırşehir, Kütahya, Manisa, Nevşehir, and Yozgat. Total installed capacity of all GDHSs (Geothermal district heating system) is 197.750 Resident Equivalent (RE) (1 RE=100m^2) and capacity in use is 127.678 RE [5].

1.1. Case Study

This study focuses on the performance analysis of the thermal insulation of district heating system components and Balcova-Narlidere Geothermal District Heating System (BNGSHS) - Izmir-Turkey is chosen as a case study. İzmir Geothermal Energy Industry Inc. has been operated in the system since 1996. The system provides heating and domestic hot water services to Balcova and Narlidere towns. Today, in Balcova, 85% of the district area and 15% of the Narlidere district area are provided with heating services and hot water. The area where district heating services are provided has reached the size of approximately 38.460 RE, as reported in 2022 [6]. Total current installed capacity of the system is 145 MW$_{th}$. With this size, it is the largest district heating system in Turkey and one of the largest in the world. The subscribers to the system are thermal tourism facilities, hospitals, universities, dormitories, faculties, and conservatory settlements.

Figure 1 exhibits the simplified flow diagram of the BNGDHS, which consists of three loops, namely geothermal, city distribution, and building loops.

Geothermal loop: Geothermal fluid from production wells at 110-120 °C is directed to a heat exchanger (HEX) and transfers its heat to the distribution system, including clean water. Then, 95% of geothermal fluid at 55-60°C is reinjected back to the reservoir by reinjection wells, while 5% is used in thermal tourism facilities.

City distribution loop: A primary geothermal fluid is utilized to heat the secondary district heating loop in heat exchanger centers. The water in the distribution system serves as both heating and domestic hot water.

Building loop: Additional HEX systems are installed at the bottom of the facilities.
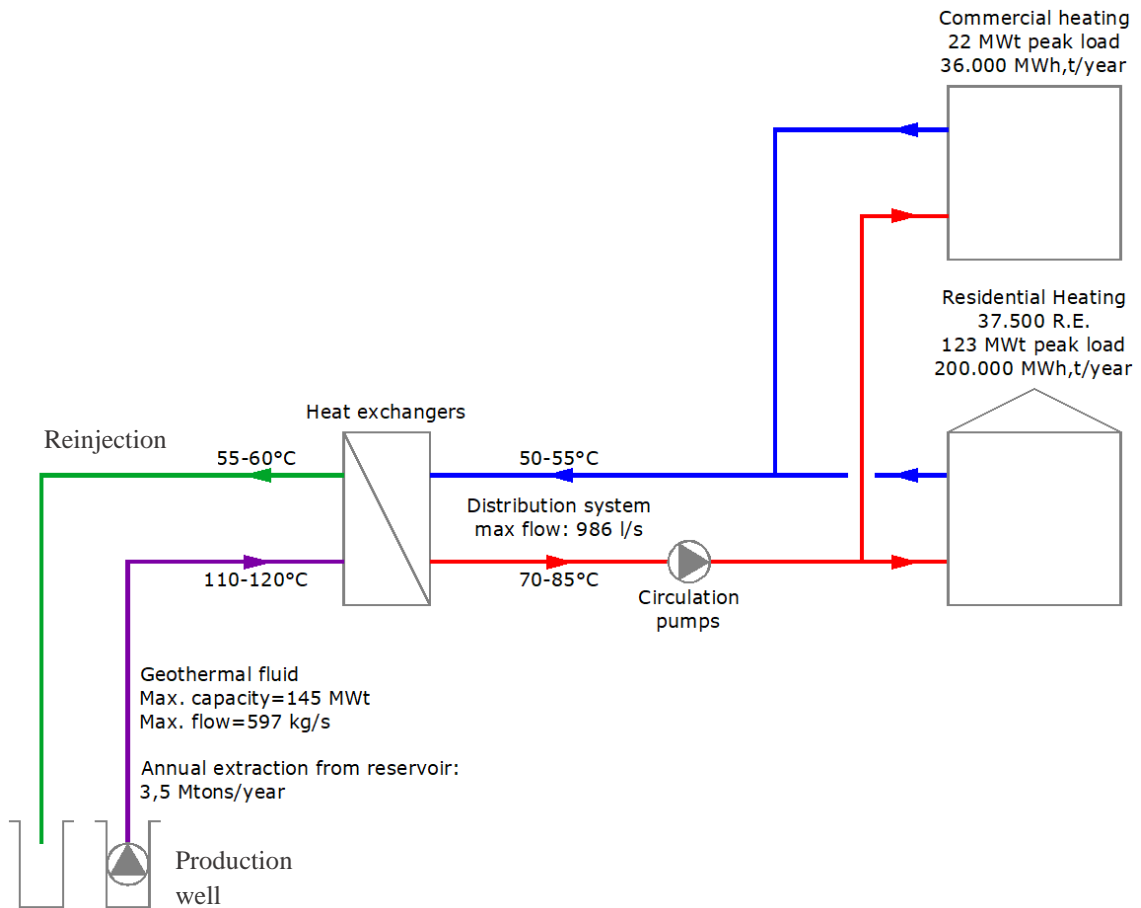
Figure 1. Flow diagram of BNGDHS [5].

İzmir Geothermal Energy Industry Inc. has 13 production wells, 5 reinjection wells, and 4 observation wells, as shown in Figure 2. Also, the company has 13 heat centers and two pump stations [7]. In Figure 2 each color shows different heating cycles and heat centers.

İzmir Geothermal Administration Building has a geothermal absorption cooling unit with a cooling capacity of 210 kW$_{th}$ [5]. It is the country's only known geothermal absorption cooling system.
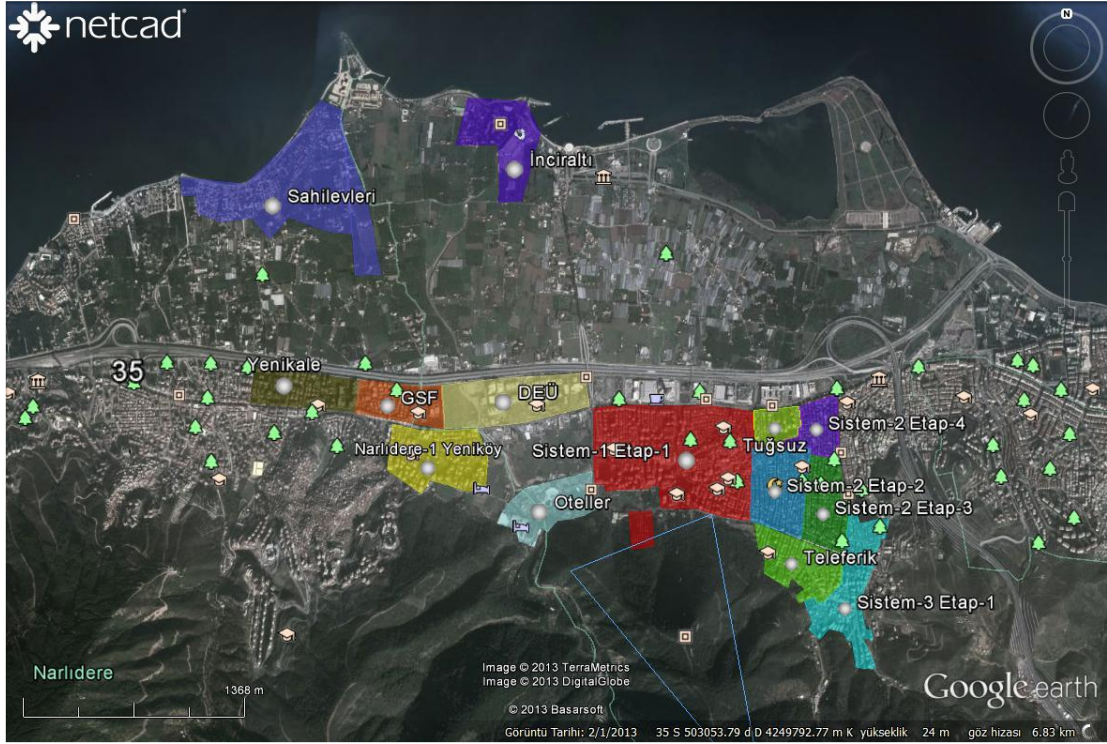
Figure 2. The area of district heating operated by İzmir Geothermal Inc. [5].

1.2. Motivation of the Study

The entire piping system on the city distribution loop is approximately 450 km. About 440 km of piping system is located underground, remaining 10 km are aboveground. Heat losses occur since the hot water travels such a long distance and also in the heat centers. There are also heat exchangers and valves under buildings. Apart from the pipes, heat losses occur from these equipment as well. The pipeline is located both underground and above ground. Underground pipes have some difficulties; corrosion, decay, the collapse of the pipes; a problem in the pipeline is complicated to understand, high maintenance cost, and heat losses. The heat and energy losses in the pipelines used to transfer the water from the well to the heat exchanger rooms in the heating system are significant. These heat losses may occur in pipes, pipe bends, valves, and heat exchangers.

In İzmir Geothermal Energy Inc., pre-insulated steel pipes are used in the underground piping system, and rock wool is used for the steel pipe insulation in the aboveground system. Rock wool is used because it can be used at higher temperatures than many thermal insulation materials, can be used easily in pipe applications, and is more affordable than other insulation materials. However, the performance of rock wool

6

deteriorates over time due to water leakage. Rock wool blankets have been used in heating centers for about eight years. This study aims to investigate and examine the insulation properties of rock wools and aerogels, understand whether aerogel blankets are useful for geothermal district heating systems, and analyze thermal performance analysis. Aerogel insulation blankets are tested in place of rock wool in this study. Two significant points for thermal insulation are the thermal conductivity of the material and the non-wettability profile. The continuation of this chapter contains information about rock wool and aerogels.

1.3. Rock Wools

Mineral wool is a fibrous mineral material, resembling loose wool or cotton in appearance, which is made by blowing a jet of air or steam through molten slag. It consists of fine, interlaced fibers composed principally of silicates of calcium and aluminum together with other minor constituents. Because of the high percentage of dead air space in a given volume of wool, it is used extensively for sound and heat insulation [8].

Mineral wool can be classified into three varieties based on the raw material used to make it. Rock wool, slag wool, and glass wool are the three types. Most rock wool is manufactured from natural siliceous limestone or calcareous shale.

Rock wool is a man-made inorganic fiber derived from basaltic (igneous) rock that is heated and melted at a high temperature in a furnace to produce a homogenous mass spun and turned into fibers with a non-fibrous melt droplet known as a shot. Rock wool is used as thermal and acoustic insulation material [9]. This production method of rock wool is kind of like making cotton candy. In the cutting section of production, rock wools could be in different sizes and shapes for various types, such as blankets or boards. In Figure 3, rock wool blanket is shown.

Some of the usage areas of rock wools are; roof and floor insulation, wall heat insulations, fire protection, acoustic insulation, and HVAC (Heating, Ventilating, and Air Conditioning) insulation.

Figure 3. Rock wool blanket [10].

Some advantages and disadvantages of rock wool;

Advantages of rock wool:

- Holds an incredible amount of water and provides a buffer against power outages and pump or timer failures.
- Always holds at least 18% air. It provides sufficient oxygen to the root area, makes watering less likely, and affects heat transfer.
- Low thermal conductivity value makes it a good thermal insulation material.
- It's so well bound that it doesn't spill.

Disadvantages of rock wool; difficult to dispose of, and if buried, it will last indefinitely. Fiber and dust from rock wool are dangerous for the lungs, and it is highly recommended to wear a dust mask to prevent problems.

1.3.1. Thermal Conductivity and Hydrophobicity of Rock Wools

The concept of thermal conductivity depends on the physical and chemical structure of a material. It is the expression of how much the material conducts heat. And heat transfer coefficient is proportionality constant between heat supplied and thermodynamic driving force of heat flow through the per unit area with change in pipe surface temperature. The constant of proportionality k or λ is the thermal conductivity.

Rock wool exhibits hydrophobic properties, but when it is under load or exposed to large amounts of water, it gets wet, can be destroyed, and permanently decreases thickness. Since water is a good conductor, it reduces the insulation property of the material as long as it is located between the rock wool fibers.

Although the porous structure and high thermal stability of rock wools seem promising, the rock wool cannot be used directly due to its weak water repellence. A thin layer of covering material is used [11]. It must be protected from water and steam condensation. If it gets wet with water, its thermal conductivity increases and the material's structure begins to deteriorate.

1.4. Aerogels

Aerogels are also called 'Frozen Smoke' and has recently been used for many purposes. Aerogel is a nano-porous material with high specific surface area, high porosity, low density, low dielectric constant, and excellent thermal insulation properties. Due to their extremely high porosity, they manifest very good thermal insulation with low thermal conductivity; they are used in insulation, aviation and space applications. Also, aerogels are used for catalysts, adsorbents, sensors, fuel storage applications, and ion exchange applications due to their porous structure. Being transparent is one of the advantages of aerogel. This feature allows the use of aerogels in optical applications and detectors.

Aerogel usage areas;
• Insulation
• Thermal insulation material
• Superinsulation material
• Acoustic insulation material
• Optical applications
• Biomedical applications
• Petrochemical facilities
• Pharmaceutical applications
• Space applications
• Speakers

• Art

• Chemical sensors

• Electrical applications

Aerogels as final products can be found in different forms; powdered aerogels, granular aerogels, blanket form, panel form, and blocks (monoliths). Different forms of aerogels are represented in Figure 4.
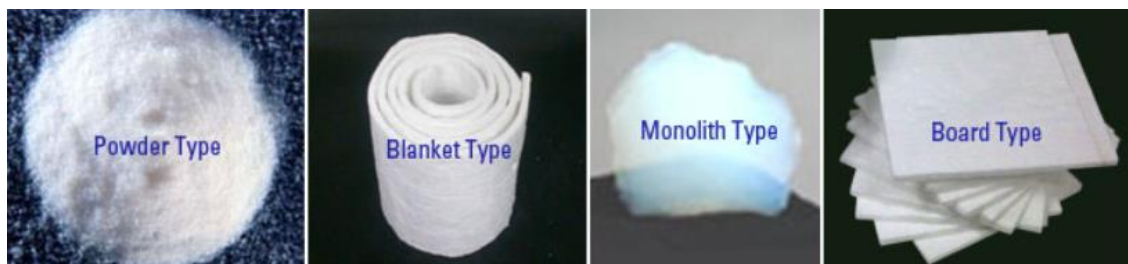
Figure 4. Some of the silica aerogel products [12].

1.4.1. Thermal Conductivity of Silica Aerogels

Heat flows from hot medium to cold medium. Figure 5(a) represents how heat flows from hot medium to cold medium in aerogels. Heat transfer occurs in three ways; conduction, convection, and radiation. Conduction is the heat transfer between solid molecules, which are the SiO_2 in the silica aerogels. Convection is the heat transfer between liquids and gases, which is the air in the silica aerogels.

Conduction is a better way of transferring heat than convection; solid intermolecular interaction is stronger than fluid intermolecular interactions. Almost 99% of the silica aerogel molecule is the air, and it is known that air does not transfer heat well [13]. While the solid body of the aerogel is very small due to the liquid part, useful cross-sectional area is minimized for transferring heat by the conduction. Since there is little way to transfer heat by conduction, the thermal conductivity of the silica aerogels is very low. There is no opportunity for conduction. A sketch of the cross-sectional area of silica aerogel shows the principle and why the thermal conductivity is low (Figure 5(b)).

In applying thermal insulation materials, the top of the insulation material is covered with materials such as a jacket with aluminum to minimize the movement of the air and minimize convection and protect the insulation materials from any mechanical damage.
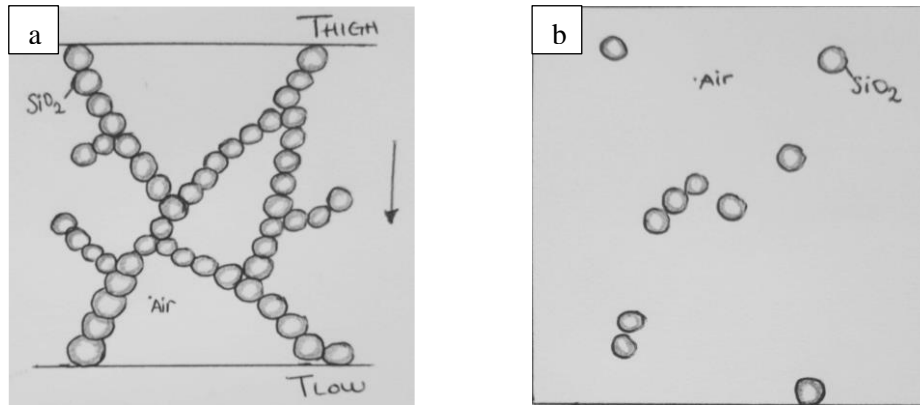
Figure 5. (a) sketch of the molecular heat transfer in silica aerogels; (b) sketch of cross-sectional area of aerogel.

1.4.2. Hydrophobicity of Silica Aerogels

Silica aerogels prepared from TMOS or TEOS have Si–OR and Si-OH groups. The Si-OH groups render the aerogels hydrophilic. The Si-OH groups can undergo strong hydrogen bonding with water [14].

Some silica aerogels are so hydrophilic as to be hygroscopic. Significant uptake of water by silica aerogels in humid environments results in the aerogel materials becoming cloudier with time and even fragmenting; this complicates the use of aerogel materials for thermal insulation [15]. In order to use silica aerogels in thermal insulation processes, silica aerogels are impregnated with glass fibers and blanket forms are formed.

Degree of hydrophobicity of the surface can be measured by many techniques such as; water uptake measurements and contact angle measurements.

- Water uptake measurements: One method used to assess the degree of hydrophobicity is to expose an aerogel to a humid environment and monitor the increase in the mass of the aerogel with time. If an aerogel is hydrophilic, its mass will increase significantly due to adsorbed water [14].

- Contact angle measurements: A small drop of water is placed on the surface of interest using a small-gauge hypodermic needle, and an image is taken off the drop. The contact angle is the droplet's angle with the surface [14].

Hydrophobic aerogels are used in thermal insulation, transparent window systems, environmental clean-up, and biological applications.

This thesis includes 6 Chapters. In Chapter 2, aerogels, types of aerogels, production of aerogel blanket, and characterization methods are given. Chapter 3 is stated for the literature survey. In Chapter 4, the materials and methods section is given for the characterization of aerogel blankets, rock wools, and energy analysis. Results and discussions for all characterization methods and energy analysis are in Chapter 5. Lastly, in Chapter 6, the thesis is finalized with a conclusion.

CHAPTER 2

AEROGELS

The term aerogel refers to a gel introduced by Kistler in 1932 and whose liquid was replaced by a gas without breaking the network of gels and solids [16]. Wet gels were dried by evaporation, but Kistler applied a new supercritical drying technique. With this technology, the liquid impregnated in the gel was converted to a supercritical fluid and then evacuated. In practice, supercritical drying consisted of heating the gel in an autoclave until the pressure and temperature exceeded the critical temperature (T_c) and critical pressure (P_c). Then, aerogels represent dry gels with a huge relative or specific pore volumes, but the values of these properties depend on the properties of the solid, and there is no official convention [14].

Aerogels are produced with the sol-gel process. The illustration of production process of aerogel is given in Figure 6.
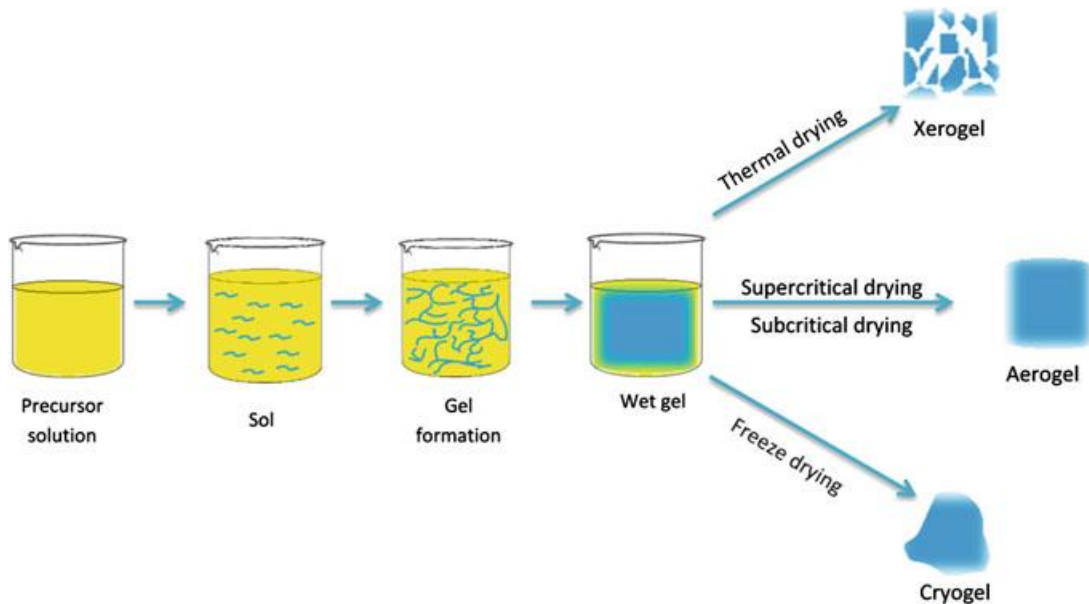
Figure 6. Illustration of sol-gel process [17].

Steps of the sol-gel process;

- Sol preparation: A colloidal suspension is formed due to the dispersion of solid nanoscale particles derived from a precursor material within a solvent.

The precursor is primarily silicon alkoxide and is available in high purity, but potassium silicate is very difficult to purify. Aerogels were obtained from three different precursors of TEOS (tetraethoxysilane), TMOS (tetramethoxysilane), and PEDS (polyethoxydisiloxane). TMOS undergoes faster hydrolysis than TEOS. MTES (methyltriethoxysilane) has been used for more flexible networks with a larger surface area than TEOS. The addition of methyltrimethoxysilane (MTMS) to TMOS increases the hydrophobicity of the aerogel [18].

- Sol to gel transition (gelation): Cross-linking and branching particles occurs due to adding an acid or a base catalyst, which initiates polymerization forming an interconnected chain structure.
- Aging of the gel: The gel is aged in its mother solution to increase its backbone and mechanical strength.
- Drying of the gel: The solvent is removed from the pores of the gel in a manner deterrent gel fracture [19].

There are mainly known three different drying types. They are; ambient pressure drying, supercritical drying with CO_2, and freeze-drying. They all work in different conditions, and products are different (Table 2). During the drying process, cracking of the gel network occurs due to capillary forces set up in the fine pores by the liquid-vapor interfaces [20].

Table 2. Drying methods, conditions and effects for aerogels [15].

Drying method	Drying condition	Effects
Ambient pressure drying	Atmospheric	'Xerogels' Causes significant shrinkage
Supercritical drying with CO_2	Supercritical State	'Aerogels' High surface area and volume
Freeze drying	Frozen	'Cryogels' Mostly mesoporous

Xerogels are obtained when the liquid phase of a gel is removed by ambient pressure drying. It may keep its original shape, but it frequently splits due to the significant shrinking that occurs while drying. Mostly has porosity between 5 and 50%.

Supercritical drying results in an aerogel. The supercritical drying method avoids the liquid/vapor boundary line by bringing the solvent above its supercritical point and then removing it from the sol-gel matrix as a supercritical fluid with high-temperature high pressure [14]. Figure 7 shows the representation of the supercritical drying state.
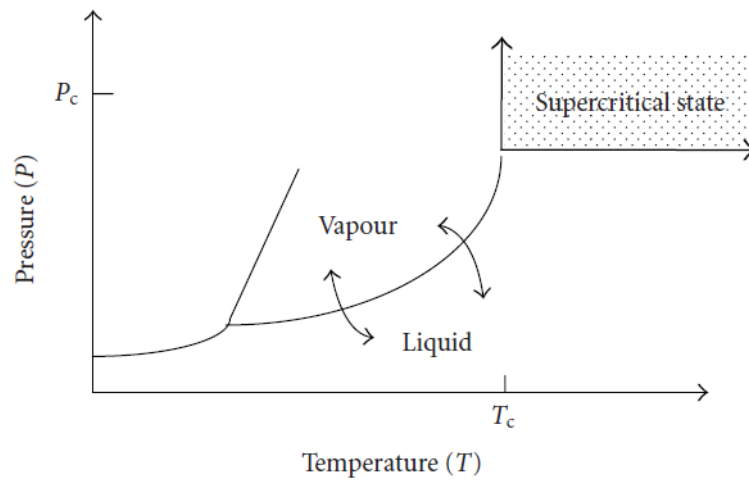
Figure 7. Representation of supercritical state at the pressure-temperature correlation for solid-liquid-vapor phase equilibrium diagram [15].

Freeze drying wet gel results in a cryogel. The result is an opaque aerogel powder. This technique removes excess solvent through sublimation. The wet gel is "frozen," and the solvent can sublimate at lower pressures [21].

2.1. Aerogel Types

Aerogel types could be categorized by the significant components such as precursors. Different kinds of aerogels are shown in Figure 8.
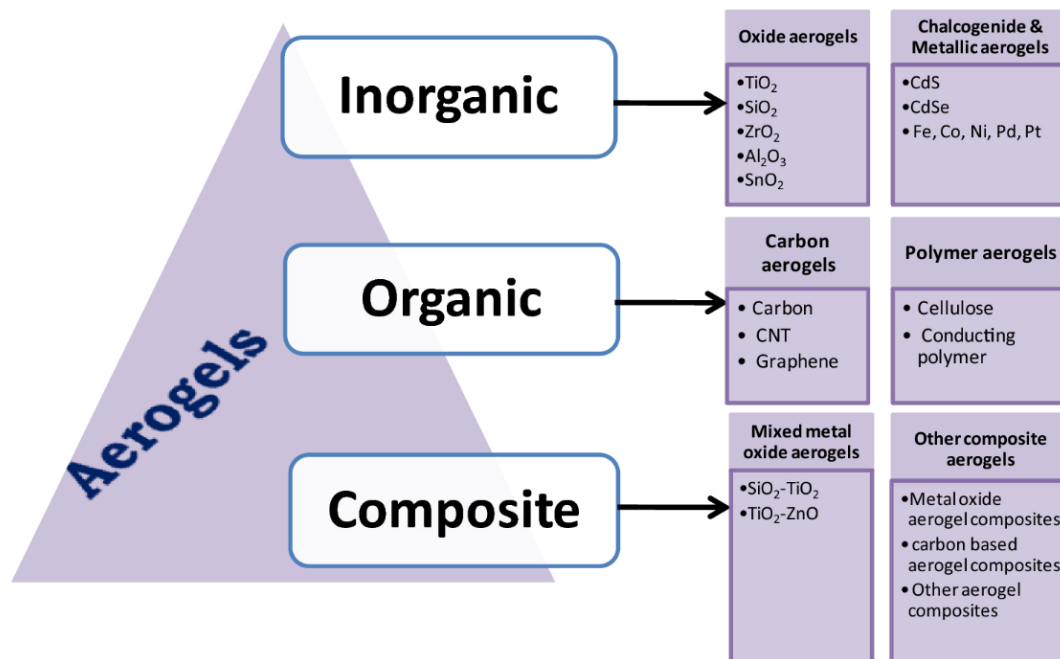
Figure 8. Types of aerogels [16].

As inorganic-silica based aerogels, silica aerogels are amorphous materials. They usually have a pore volume of more than 90% of their total monolith volume. Silica aerogels tend to be mostly mesoporous, with interconnected pore sizes typically in the range of 5-100 nm and average pore diameters of 20-40 nm [14]. The main precursor of silica aerogel is silicon alkoxide [22].

A lot of studies are being done today on inorganic-non silicate aerogels. These aerogels are prepared with different components and by using different methods. Some of the inorganic-non silicate aerogels are; ZrO_2 and TiO_2 aerogels. Non-silicate aerogels are mostly used in space applications [14].

Many studies are being done to develop organic aerogels with various parameters. Commonly known organic-natural and synthetic aerogels are carbon, fibrous cellulose aerogels, cellulosic aerogels, and polyurethane aerogels. For example, carbon aerogels are produced in the same way as other aerogels, except for some differences. The main difference in the carbon aerogel production process is the pyrolysis step which is also called carbonization. Carbon aerogels are brittle and fragile as SiO_2 aerogels. Therefore, they cannot be used directly as thermal insulation material without any cover material [15].

2.2. Silica Aerogels

The chemical representation of silica aerogel is SiO_2 which calls as silicon dioxide. Silica aerogels are made from silica; if going deeper, silica aerogels are made from silicon. Silicon is a material that can be easily found on Earth. Mostly silicon can be found in the form of silica or silicate. Silica aerogel is chemically identical to sodium silicate (water glass) [23].

Some information about silicon and silica, such as; the picture of them, their properties, and usage areas, are represented in Table 3. The basic formulation of silica;

$$Silicon\ (Si) + Oxygen\ (O_2) = Silica\ (SiO_2)$$

Table 3. Information about silicon and silica.

	Silicon	Silica
Their picture		
What are they?	2nd most abundant element on Earth after Oxygen	Produced from the reaction between Silicon and Oxygen
Properties	- High melting point and boiling point - Bluish-grey metal appearance	- High purity - Heat resistant - High transparency
Usage areas	Semiconductors in computers and other electronics	- Glass - Ceramics - Optical Fibers

Aerogel sketched in Figure 9 shows the network of the silica aerogel.
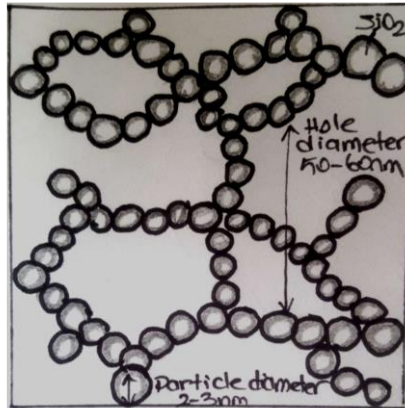
Figure 9. The illustration of the network of the silica aerogels.

2.3. Silica Aerogel Blankets

Silica aerogel blankets are the most suitable silica aerogels for many industrial applications. The production process of aerogel blankets is a bit different from granular or powdered form aerogels. It is produced by adding the liquid-solid solution to the fibrous batting [24]. The basic product is made up of a silica aerogel infiltered into the fiber blanket. Infiltration of aerogel is done by soaking the 'sol' into the fiber blanket, then 'sol' to 'gel' conversion to get fiber blanket–gel sheet. This gel blanket is then dried super critically to get the aerogel blanket. Infiltration of aerogels into the fiber blankets can possess up to 90% aerogel between the layers [13]. Figure 10 presents the production line of the aerogel blanket.

An aerogel blanket is a combination of granular silica aerogel and non-woven reinforcement that turns fragile aerogels into a durable, flexible/solid material. The primary market sector for aerogel enhanced products is the oil and gas industries, which mainly use aerogel enhanced blankets for pipe insulation. However, the aerogel market for the construction and construction industry is expected to increase more than any other sector in the next decade [26].
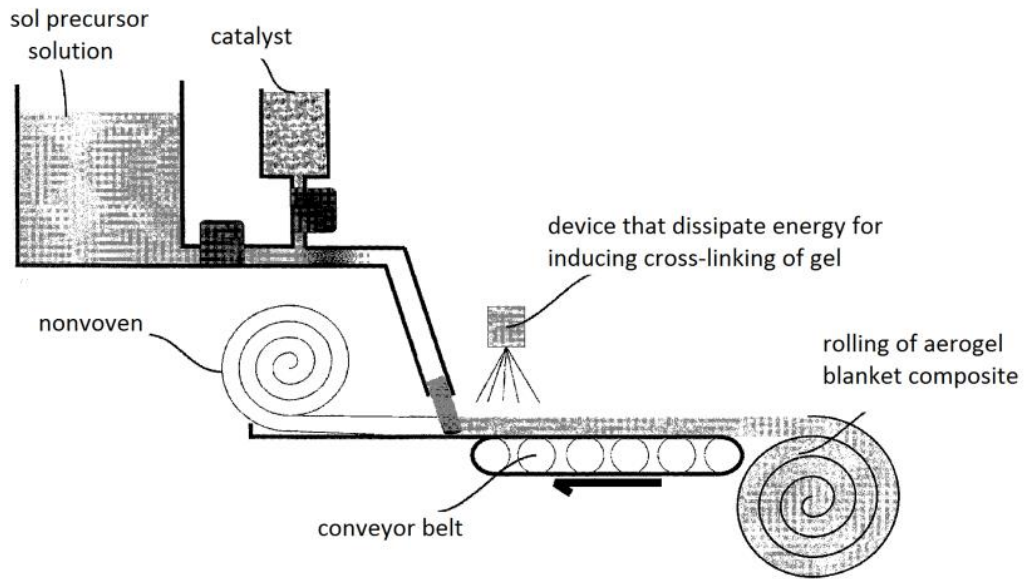
Figure 10. Scheme of the production of aerogel blanket [25].

Silica aerogel blankets are prepared by a discontinuous one step process, using different textile fibers (glass, partially carbonized acrylic, polyester microfibers, etc.) as a fiber reinforced component. Aerogel blankets mechanical and thermal insulation properties can be changed with additives such as fiber types, blanket thickness, and metal powders [23]. Figure 11 shows the silica aerogel-based blanket.

Figure 11. Picture of the silica aerogel-based blanket.

Aerogel particles are attached to glass fibers, but there is no information that aerogel particles attach homogeneously. Fibers in the form of blankets are also not homogeneously dispersed. The drawing shown in Figure 12 depicts a model of the heat transfer pathways. When the aerogel is added to the system heat transfer along R3 and

R4 is significantly decelerated as aerogel is best known for its extremely low thermal conductivity.
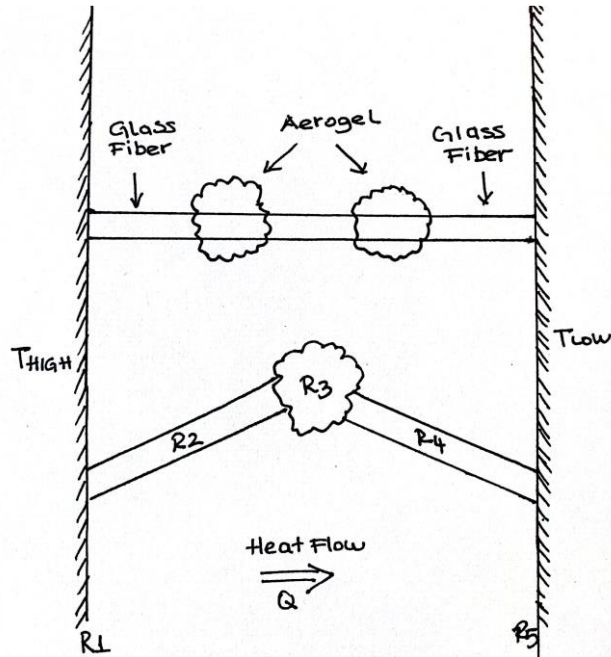
Figure 12. Model for the heat transfer process of aerogel-based insulation blankets.

Blankets are used with a protective cover. As shown in the Figure 12, the resistances R1 and R5 symbolize the cover material. R2 and R4 resistances represent the glass fiber, and R3 symbolizes the resistance of the aerogel particle. The internal insulation mechanism of the aerogel insulation blanket can be expressed by Equation 1.

$$R_{Tot} = R_1 + R_2 + R_3 + R_4 + R_5 \qquad (1)$$

Blanket type silica aerogels can be used in; petrochemical facilities, pipe and boiler insulation, heat insulation of land and air vehicles, refrigerated vehicles, internal insulation of small appliances, hot and cold-water tanks, insulation of high-temperature ovens, roof and ground insulation, wall insulation; in between bricks or panels, and fuel tanks.

CHAPTER 3

LITERATURE SURVEY

Geothermal energy is heat energy obtained from hot water, steam, and dry steam and accumulating in the depths of rocks.

The use of geothermal energy; generally, varies depending on the temperature and capacity of the geothermal resource. However, it has a wide range of uses. The main ways of using geothermal energy are; electricity generation, indoor heating, thermal tourism, agricultural use (green house), industrial use (process water heating, drying), absorption cooling, and dry ice production.

3.1. Geothermal District Heating

Geothermal energy utilization can be categorized into two groups with regard to the temperature of geothermal resources: electricity generation and direct use [27].

Generally, geothermal fluid with low temperatures is required for direct use. Geothermal resources having fluid temperatures between 90 and 150°C are suitable for district heating. Heat is distributed to many individual houses or blocks of buildings from a central location through pipes, as shown in Figure 13.

Heat centers are located near the production and reinjection wells. The hot geothermal water is drawn to the earth with the help of a pump. With the heat exchanger in the heat center, the mains water is heated without mixing geothermal water into the mains water. The heated mains water is distributed to the residences. After the mains water is heated, the geothermal water cools, and with the help of the reinjection pump, cooled geothermal water is reinjected into the underground.
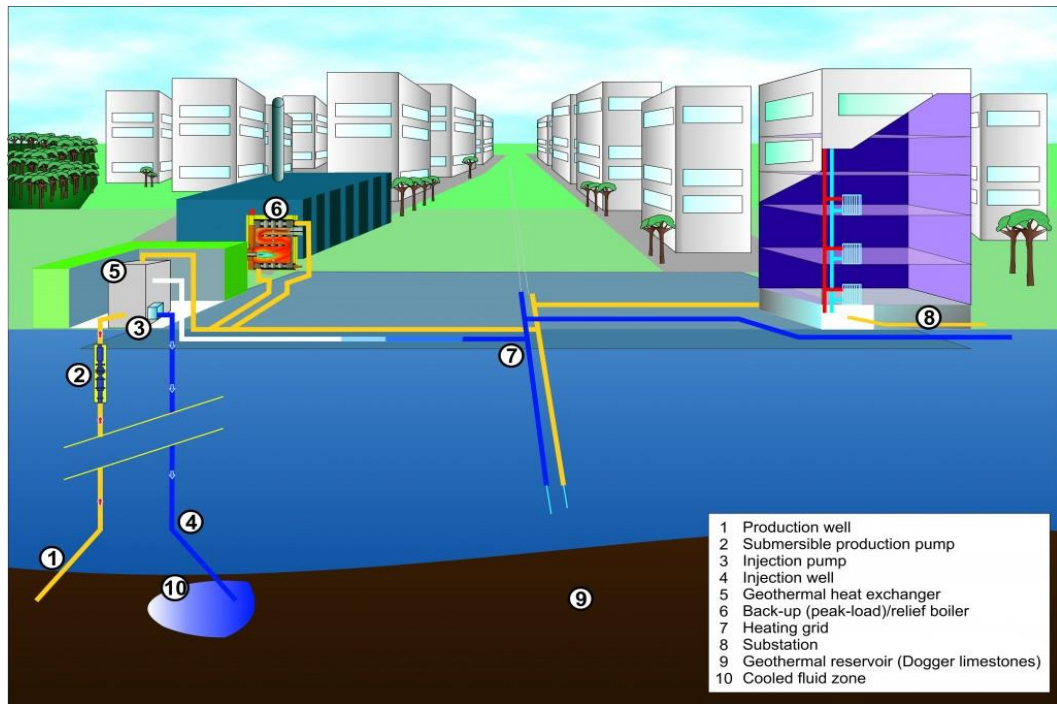
Figure 13. Scheme of the geothermal district heating system [28].

District heating provides many advantages, such as the easy use of various fuels, especially the control of air pollution, the fire hazard being far from the settlements, and the more efficient use of energy. Keçebaş et al. (2011) performed the work for calculation of the optimum rock wool insulation thickness of pipes used in district heating pipeline networks in Afyonkarahisar/Turkey, energy savings, and payback times for five different pipe sizes and fuel types [29].

Comakli et al. (2006), examined the losses in the system by making energy and exergy fields in the district heating system of Ataturk University; they reported that the 12 km pipeline's total energy loss is 64656 kJ, and exergy loss is 55546 kJ [1].

Baker et al. (1997), conducted an energy analysis of an airport district heating system in the United States. In this study, they carried out the optimization study of the pipe distribution networks with the computer program they developed. They determined that a significant amount of heat losses occurred due to the very old and complex piping, and re-determined the economical insulation thicknesses and optimum operating temperatures for the system [30].

Böhm (2000) determined in his theoretical work, the heat loss relations for different pipe insulation combination situations (insulated pipe, insulated pipe, two pipes

insulated separately or in case of two pipes insulated together, and the depth of burial of pipes in the ground) in district heating systems in buried hot water pipes. They made calculations by obtaining [31].

Adamo et al. (1997), in their study in Italy, calculated the optimum pipe diameters and insulation thicknesses in a district heating system with a three hundred (300) km pipe distribution network using the thermo economic analysis method. It has been revealed that 55380 $ can be saved per year from the pipe distribution network if the optimum values are followed [32].

Gustafson (2000), in his study, optimized to reduce the energy used in old buildings and developed a simulation program for this. Using this program, he made a life-cycle cost comparison in heating systems. The most important result emphasized here is to re-insulate the buildings in order to reduce the operating costs in district heating systems and to design the buildings in a way that minimizes heat losses [33].

3.2. Aerogel Insulation

Beginning from the first global oil crisis, all resources for the chemical and energy industry have been changed by modern society for cheap energy and resources. Global energy strategies changed. Thermal insulation reduces energy usage. Applying aerogels as a thermal insulation material is a method to decrease the emission of greenhouse gases. In the building industry, space-saving is the most important reason for the use of superinsulation. Typical cases are interior insulation solutions for building retrofit and thin façade insulation for the renovation of old historically important buildings, side balconies, and roof balcony constructions [34].

Silica aerogels are not suitable for use alone in thermal insulation because they are fragile and brittle. Accordingly, fibers were added to improve the strength of the aerogel. Table 4 shows the advantages and disadvantages of aerogel insulation.

Table 4. Advantages and disadvantages of aerogel insulation.

	Advantages	Disadvantages
Aerogel insulation	Relative low thermal conductivity	Uncertain long-term physical properties
	Possible transparency	Energy-extensive and expensive production process
	On-site use similar to traditional materials	Uncertain health risks

The main application area of aerogel materials is in the buildings, and different focus areas in the buildings are:

• Renovation of historical buildings

• Interior insulation and windows

• Elements of aesthetic architecture

• Balcony structures with flat roofs

Jensen et al. (2005) perform a study to investigate super-insulating aerogel window [35]. The product of their work is given in the Figure 14 and, Figure 15.

Figure 14. Examples of super insulating silica aerogels window and aerogel granulate filled glass fiber composite panels in the form of a transparent day lighting roof construction [22].

Figure 15. Example of exterior renovation house in Zurich [22].

The thermal treatment significantly affects the pore structure in aerogels, and obvious variations of pore volumes, and specific surface areas occur. It is known from the study of Nocentini et al. (2018) that the BET (Brunauer–Emmett–Teller) surface area values of aerogel insulation blankets are around $200m^2/g$ [36]. This high surface area and high porosity have been evaluated to contribute to thermal insulation. Accordingly, the thermal conductivity is changed. A lower thermal conductivity means that the same insulation is achieved with a thinner insulation layer. The overall thermal conductivity of an aerogel material is the sum of three components: conductivity by the solid phase, gas phase, and radiation [37].

An insulating layer reduces heat transfer between two work pieces held at different temperatures and thus helps to reduce energy losses [22].

Within the field of super insulating sol gel silica materials, the most recent studies concern fibrous composites such as blanket type forms. Mostly aerogel blankets are used with cover jackets to reduce the blanket from side effects.

Some parameters should be considered in thermal insulation applications using aerogel blankets as insulation material;

- Physical Parameters
  - Heat transfer coefficient
  - Water–vapor diffusion resistance coefficient
  - Low thermal conductivity
  - High thermal resistance
  - Density

- Durability
  - Water and moisture resistance
  - Resistance to chemical agents
  - Durability against atmospheric conditions
  - Durability against corrosion
  - Temperature resistance
  - Fire and heat resistance
  - Human health effects
- Easy applicable and long life
- Economic

Since the term insulation is very much in our lives, many studies have been carried out on aerogel insulation material. Different types of aerogels have been produced for use in different areas, and their characterization has been investigated. To understand that the correct insulation material is used for the system, it is necessary to measure and know the physical and chemical properties of raw materials and products of any process. Properties can be known with the help of some analyzes and techniques.

Parameters that affect aerogels' synthesis are pH, reflux time, reflux temperature, aging time, aging temperature, and drying method. After aerogel and aerogel blanket production; for characterization, the physical and chemical analysis must be done. After characterization, it can be known in which purpose and where the aerogel can be used. In many studies, many analyses have been used to characterize aerogels. These analyses measure thermal stability and conductivity, chemical bounding, specific surface area, and product volume, hydrophobicity, water vapor permeability, microstructure, and microscopic morphology of materials.

- AFM: Atomic force microscopy can check densification [18].
- BET: The specific surface area, pore size distribution, and pore volume can be measured for various samples using a nitrogen gas adsorption Brunauere-Emmette Teller apparatus [38].
- EDX: The energy dispersive X-Ray spectroscopy interested in the presence of atoms in the material.

- FTIR Spectroscopy: The surface chemical bonding states and surface modifications can be measured with the Fourier Transform Infrared Spectroscopy (FTIR) using an IR spectrophotometer.

- HFM: A heat flow meter can be used for thermal conductivity measurement [39].

- TG-DTA: Thermo gravimetric and differential thermal analyses measure the thermal stability of aerogels.

- SEM-TEM: Scanning electron microscopy (SEM) and transmission electron microscopy (TEM) are techniques that may provide information on the microstructure of aerogels [18].

- XRD: X-ray diffraction is a technique used for phase identification of a crystalline material and can provide information on unit cell dimensions.

- Silica aerogels can either be hydrophilic or hydrophobic, depending on the conditions during synthesis. The hydrophobicity is characterized by measuring the contact angle (θ) of a water droplet placed on the silica aerogel blankets surfaces with cutting.

Various analyzing methods could characterize rock wools. Siligardi et al. (2017) performed a comparative study between fiber-reinforced silica aerogel and rock wool and made some characterization analyzes such as; TGA (Thermo gravimetric Analysis), XRD (X-ray Diffractometry), FTIR (Fourier-Transform Infrared Spectroscopy), SEM (Scanning Electron Microscope), thermal conductivity analysis, and flammability test [40].

Chakraborty et al. (2016) synthesized aerogel blankets at various trimethylchlorosilane (TMCS) concentrations were characterized and compared with the blankets that did not contain aerogel against high temperature and fire protection [41].

Hoseini et al. (2016) studied theoretically and experimentally the effective thermal conductivity of two distinct aerogel blanket composites [42]. Nocentini et al. (2018) aimed to examine and describe two types of lightweight, super-insulating aerogel blankets that have been dried under ambient conditions to see if they are acceptable for building thermal insulation. As a difference, BET analysis made for pore sizes of the insulation material [36]. Lakatos et al. (2019) aimed at thermal investigations on heat-annealed glass fiber reinforced aerogel [24]. Umberto et al. (2019) aimed to characterize and compare

commercial aerogel-enhanced blankets made via supercritical drying and a new ambient pressure drying blanket [26].

Their orientations on characterization methods are given in the Table 5 given below. In Chapter 4, extensive characterization studies are given for aerogel blankets and rock wools.

Table 5. Some aerogel blanket studies.

Author(s)	Year	Characterization analysis and orientations							
		CAM (*)	D (**)	FTIR	SEM	TGA	HFM	EDX	DSC
Chakraborty et al. [41]	2016	√	√	√	√	√	√		
Hoseini et al. [42]	2016			√	√		√		
Nocentinia et al. [38]	2018	√	√	√	√		√	√	
Lakatos et al. [24]	2019						√		√
Umberto et al. [26]	2019	√	√	√	√		√		

Where;

* CAM is a contact angle meter.

** D is the density.

CHAPTER 4

MATERIALS and METHODS

In this part of the study, experiment, characterization of aerogel blankets and rock wools, interpretation of laboratory analysis, and energy analysis topics are given. Aerogel blankets were evaluated for the geothermal district heating system instead of the currently used rock wool. Rock wool and aerogel blanket samples were used to examine the thermal performances and to observe the heat losses. Glass fiber blankets could also have been evaluated, but the district heating system involving this study was not interested in these materials due to cost concerns.
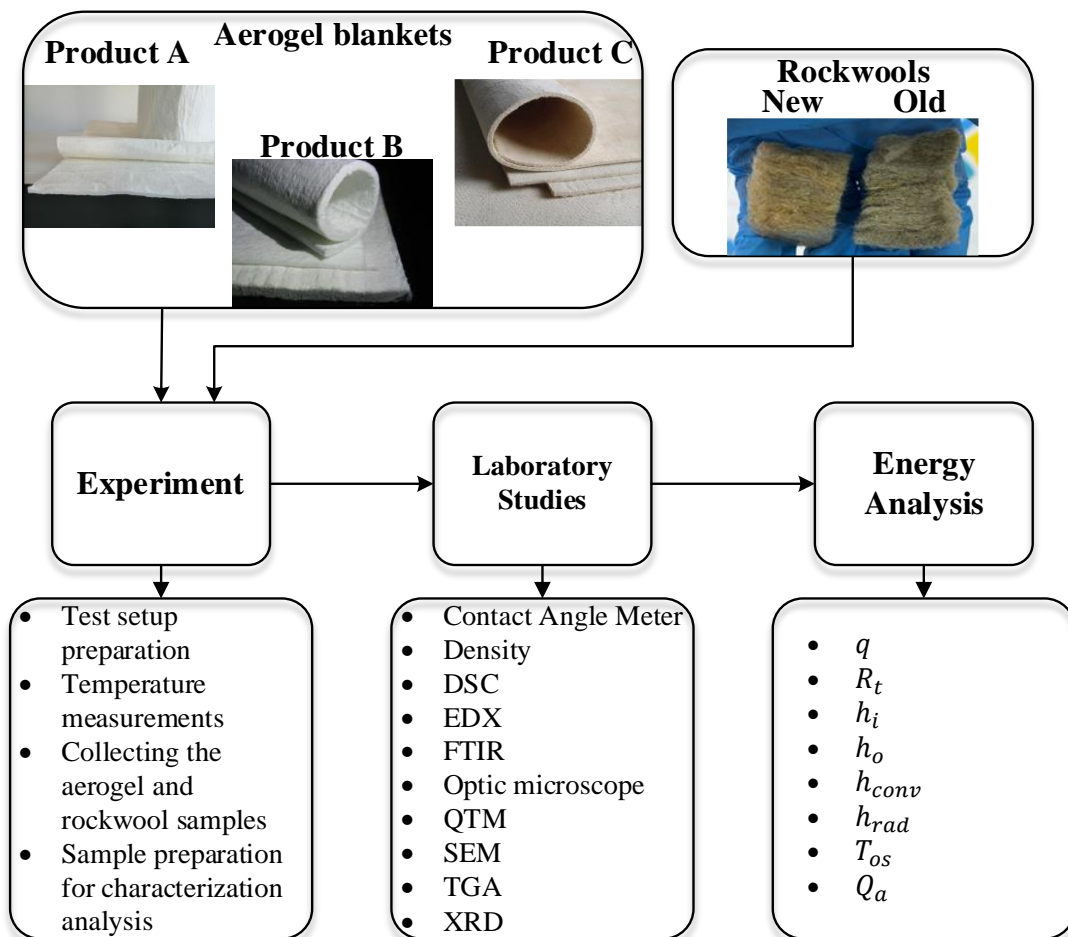
Figure 16. Schematic representation of Materials and Methods Section.

Figure 16 shows a basic schematic representation of this chapter. This chapter has three main sections: experiment, characterization, and energy analysis. All sections are explained and examined step by step in the continuation of the chapter for both rock wool and aerogel blanket samples.

Three similar silica aerogel blankets from different manufacturers were investigated; therefore, aerogel blankets were named as A, B, and C. Two rock wool samples from the same manufacturer were analyzed. One of them was used for about eight years, so that rock wool is called 'old,' and the other is newly produced and unused, called 'new' rock wool.

4.1. Experimental

In İzmir Geothermal Energy Industry Inc., a test setup is prepared for aerogel blankets in the B4A well. After the tests made for aerogel blankets, another test setup is prepared for rock wools in a well named BD11. Properties of pipes used in these wells-heat centers are given in Table 6.

Table 6. Properties of cold-drawn steel pipes in heat centers.

	B4A well	**BD11 well**
Nominal diameter	DN150 – Sch40 ANSI	DN250 – Sch40 ANSI
Outer diameter (mm)	168.3	273.1
Wall thickness (mm)	7.11	9.27
Lenght (m)	1	1

Temperature measurements were taken with Testo 925 temperature measuring device (Figure 17 and Table 7).

Figure 17. Testo 925 temperature measuring device [43].

Table 7. Technical Data for Testo 925 temperature measuring device [43].

Measuring Range	-50 to +1000°C
Accuracy	±(0.5 °C + 0.3 % of mv) (-40 to +900 °C) ±(0.7 °C + 0.5 % of mv) (Remaining Range)
Resolution	0.1 °C (-50 to +199.9 °C) 1 °C (Remaining Range)
Dimensions	182 x 65 x 40 mm
Operating temperature	-20 to +50 °C
Weight	171 g

4.1.1. Aerogel Blankets

Three different silica aerogel blankets were applied to the cold-drawn steel pipes and valves connected in parallel, with a geothermal fluid inlet at the same temperature and pressure (Figure 18). They were left to be stable after 4-5 days of exposure to operating conditions. Pressure measurements from 2 points, surface temperature from 11 points, and ambient temperature were taken on the test setup. Two of the aerogel blankets used in this study are of foreign origin aerogel blankets, and one of them is a domestic product. The average price of the aerogel blankets is $150/m^3.

Figure 18. Picture of the test setup with aerogel blankets in B4A well.

4.1.2. Rock wools

To determine the thermal performance of old and new rock wool samples, it is planned to take surface temperature measurements while renewing the insulation material in pipes and valves with geothermal fluid inlet at the same temperature and pressure.

Surface temperatures from 3 points and ambient temperatures were taken on the test setup. The old rock wool has been used for about 8 years. The test setup consists of DN250, cold-drawn steel pipes, and valves. Picture of the setup and measuring points are shown in Figure 19. The price of rock wool blanket is 500 TL/m^3.
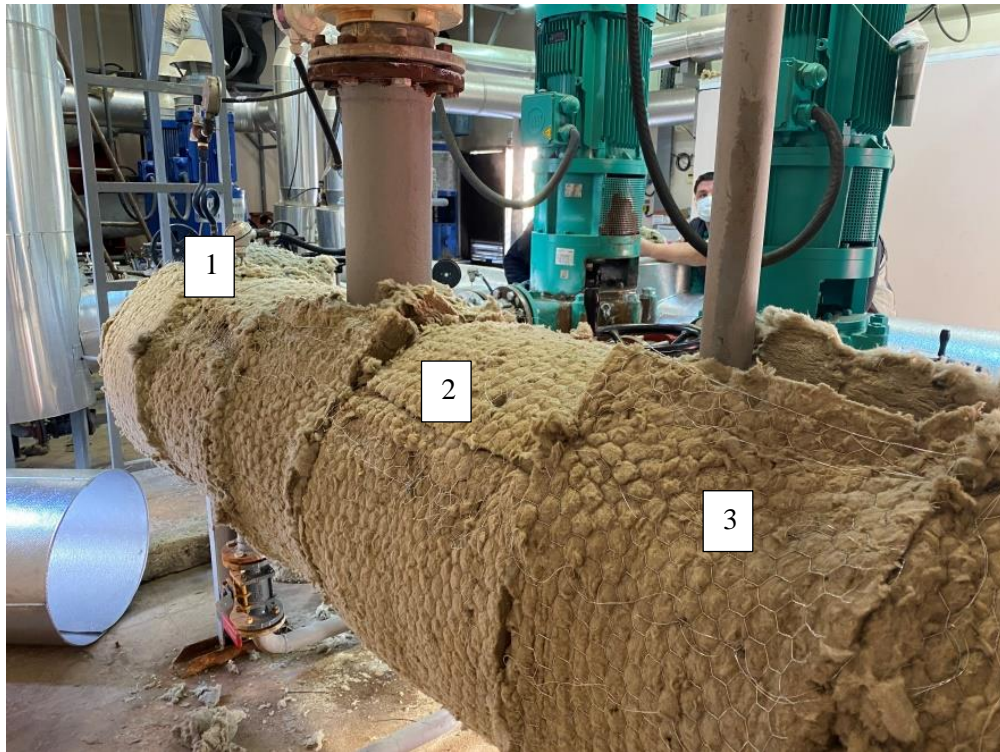
Figure 19. Picture of the test setup with rock wool and measuring points in BD11 well.

The aerogel blankets and rock wools used in the test setup were removed from the places where they were mounted and brought to IZTECH for laboratory tests. Samples were prepared by cutting them into sizes suitable for each type of analysis and separated from their cover.

4.2.   Laboratory studies

Density, thermal conductivity, thermal stability, heat transfer coefficient, specific surface area, pore sizes, hydrophobicity, microstructure, and microscopic morphology of the silica aerogel blankets and rock wools are measured to determine the best thermal and non-wetting performance with the help of some analysis methods. After sample preparations had been completed, analyses were made within the IZTECH-Integrated Research Center (IRC) body. In Integrated Research Center, CMR (Center of Materials Research), ENVIROCEN (Environment Development Application and Research Center), and GEOCEN (Geothermal Energy Research and Application Center) have some of the analysis techniques. Each analysis was performed in 3 variations, and the arithmetic mean

of the results was used; Standard deviations were also calculated for each analysis. In Table 8, this analysis, their measuring area, and the location of this analysis in IZTECH are tabulated.

Table 8. Analysis, their measuring areas, and locations in IZTECH.

Analysis	Measures	Location in IZTECH
Density Measurements	Density	Laboratory
TGA (Thermo gravimetric Analysis)	Thermal stability	CMR
SEM (Scanning Electron Microscope)	Particle size, crystal structure	CMR
Contact Angle Meter	Hydrophobicity	Laboratory
EDX (Energy-Dispersive X-ray Spectroscopy)	Chemical composition	CMR
QTM (Quick Thermal Conductivity Meter)	Thermal conductivity	GEOCEN
XRD (X-ray Diffractometry)	Phase identification	CMR
FTIR (Fourier-Transform Infrared Spectroscopy)	Chemical bonding states	ENVIROCEN
DSC (Differential Scanning Calorimetry)	Heat capacity (specific heat)	CMR / ENVIROCEN

4.2.1. Density measurements

Aerogel blanket samples of 10x10x10 mm were cut for density measurements, and rock wool samples were cut of 20x20x20 mm. In Figure 20, samples of aerogel blankets and rock wools are shown, respectively. Mass changes at a constant volume were determined for three different temperatures, and density was calculated according to Equation (2).

$$\rho = m/V \ (kg/m^3) \qquad (2)$$

In the first calculation, the samples were weighed at ambient temperature (30°C), and in the second calculation, they were heated up to 110°C in an oven, dried for 24 hours, and weighed. The third calculation was made with thermo gravimetric analyzes (TGA) after heating up to 765°C.
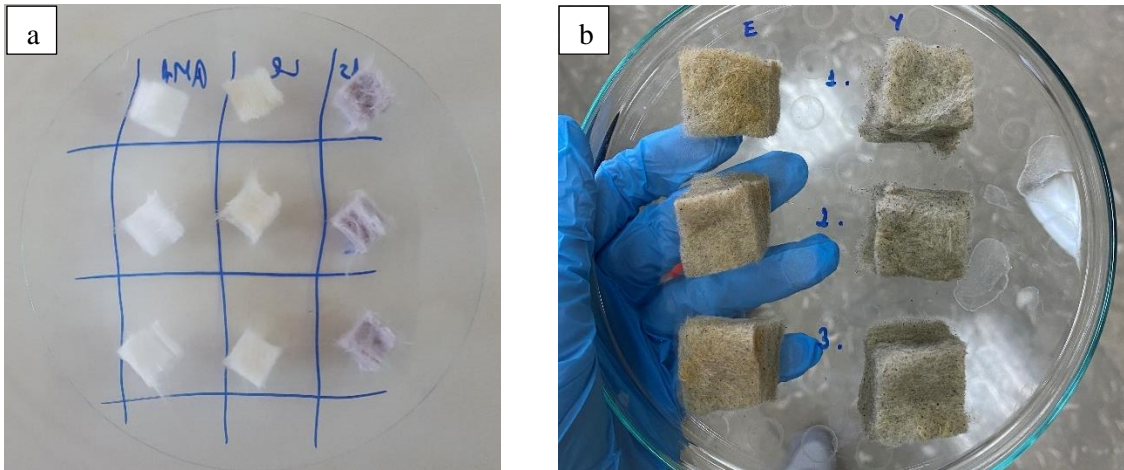
Figure 20. (a) Aerogel blanket samples, (b) Rock wool samples.

4.2.2. Thermo gravimetric analysis (TGA)

The samples were heated from 25°C to 765°C at a heating rate of 10°C/min by taking instantaneous weight measurements while hanging on a precision balance for analysis. This analysis aims to determine the decomposition reactions due to heating. Heating was carried out with 50 ml of nitrogen per minute.

The sample is heated to a certain temperature and kept at this temperature. The mass loss in the material generally occurs as a step that can be easily seen on the TGA curves. In general, the factors that cause this type of behavior are; can be listed as the volatile components existing in the material as evaporation, drying in the sample, and gas absorption.

4.2.3. Optical microscope images

All samples were viewed under a stereo zoom optical microscope. This observation aims to understand the structure of the materials before more accurate observations, such as in SEM.

4.2.4. Scanning electron microscopy (SEM) observations

SEM is used to investigate the distribution and size of particles in materials. Particles are measured in nanometers (μm). All samples were coated with a thin layer of gold in a sputter coater device before examination in the Quanta Feg 250 brand and model SEM. Then, images of the samples observed in the secondary electron (SE) mode at different magnifications were obtained. Aerogel fiber diameters and aerogel adhesions were observed.

4.2.5. Contact angle measurements

Contact angle measurements were made to determine the non-wetting properties of samples. All samples and aerogel blanket sample covers were measured in the Attension-Theta model contact angle using approximately 3μL of distilled water. For a material to exhibit non-wetting property, the contact angle is expected to be greater than 90° [44]. The larger the contact angle, the better the non-wetting property.

Hydrophobicity of materials can be measured by a method represented in Figure 21. A drop of water is put on the materials surface. Then the contact angle (θ) is measured. If the contact angle is bigger than 90°, material is hydrophobic. If smaller than 90°, material is hydrophilic, as seen in Figure 21.
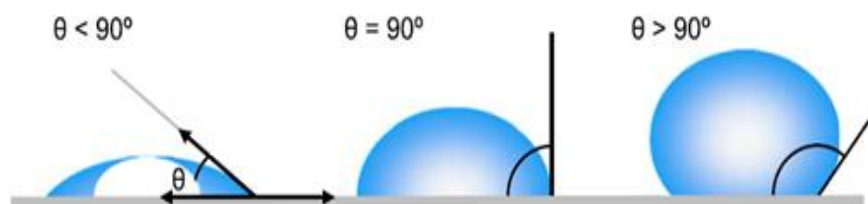
Figure 21. Hydrophobicity of the aerogel [44].

A lot of studies have confirmed that the surfaces with the water contact angle bigger than 150° is called as 'superhydrophobic' or 'ultra-hydrophobic' surfaces.

4.2.6. Energy dispersive X-ray (EDX) observations

EDX observations with a high-speed electron beam in the SEM device give an idea about the elemental chemical composition of the region under investigation. The EDX detector is used to determine the chemical composition of the sample. (EDX Oxford Inc.-Aztec).

Analyzes were made for aerogel particle and fiber individually for each sample.

4.2.7. Thermal conductivity analyzes

KEM-QTM 500 model device was used for heat thermal conductivity measurements. The device has a standard of ASTM 1113-90. QTM is the quick thermal conductivity meter. The thermal conductivity is indicated by k (W/mK).

4.2.8. X-ray diffractometry (XRD) observations

XRD is used for phase identification of a substance considered to be crystalline/amorphous. So, XRD is a form of analysis used for crystalline substances. XRD can follow all the crystallization events starting from the first nucleation to the final crystallization phase in supercritical drying, so the structural changes of the material in this process. With the increase in additives and fibers, peaks can be observed. Also, this situation may weaken the homogeneity of the material; as the heterogeneity increases, the number of peaks increases. Cu Kα radiation was used.

4.2.9. Fourier transform infrared spectrometry (FTIR) observations

FTIR is used to characterize organic or inorganic compounds. Analysis observations are provided by the absorption peaks corresponding to the frequencies

formed by the vibration of the bonds between the atoms that make up the material. Each material has its peak points.

4.2.10.   Heat capacity (specific heat) measurements

Heat capacity (C_p) measurements were measured by Differential Scanning Calorimetry (DSC). The measurements were started at -10°C for each sample, increased by 10°C per minute, and completed at 300°C. C_p values can be calculated depending on the operating temperature. Heat capacity values were calculated for 110°C, one of the temperatures used in the density calculation, representing the average geothermal operating temperature. Heat capacity can be defined as the amount of heat required to raise the temperature of a substance/material by 1°C. The heat capacity is a parameter that depends on the heat transfer coefficient. Materials with high thermal conductivity heat up and cool down quickly. Thermal conductivity and heat capacity are inversely proportional.

4.3. Energy Analysis

The main purpose of this thesis is to determine the energy performance of insulation materials. Energy analysis was carried out to observe the effects of the physical and chemical properties of rock wool and aerogel samples on heat losses. This analysis is a heat loss calculation. Energy analysis directly affect the cost and payback period of thermal insulation applications. There are some parameters of energy analysis; it is important to know the surface temperature of insulation materials, know the composed heat losses, and know how much energy is conserved.

There are two important parameters in insulation materials; optimum thickness and use of correct material. Increasing the thickness of the insulation material will reduce air pollution and increase energy savings. However, an insulation thickness that provides zero heat loss is neither practical nor economically possible [46].

In this study, EES (Engineering Equation Solver) software [47] is used for modeling energy analysis. Static energy analysis was performed with EES. The EES is a

general-purpose equation solver that can numerically solve thousands of connected non-linear algebraic and differential equations. This software solves differential and integral equations, optimizes, performs uncertainty analysis, performs linear and non-linear regression, checks units, checks unit integrity, and produces publication-quality graphs. An important feature of EES is a highly accurate database of thermodynamic and transport properties provided for hundreds of materials for use in the ability to solve equations.

EES preserves thermodynamic properties and eliminates the need for repetitive hand problem solving through code that recalls properties with specified thermodynamic properties. EES runs an iterative solution and eliminates the tedious and time-consuming task of capturing thermodynamic properties using built-in functions [47].

Heat is the energy transferred by a temperature differential between two systems or between a system and its surroundings. The second law of thermodynamics states that heat must be transported from hot to lower the temperature. Heat, transfers in several ways; conduction, convection, and radiation. Thermodynamic expressions (Table 9) used during the energy performance analysis and figure for insulated pipes (Figure 22) are given below.
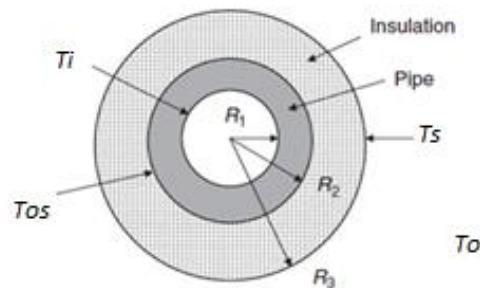
Figure 22. Sketch of the insulated pipe

Assumptions were made for the energy analysis are;
- Geothermal fluid is assumed as pure water,
- The temperature, velocity, and pressure of geothermal fluid are assumed constant,
- Process is assumed as steady-state, steady-flow so the air pressure and temperature are assumed constant,

- The thermodynamic properties of air such as thermal conductivity (k), viscosity (μ), expansion coefficient (β), kinematic viscosity (ν), specific heat (C_p), and thermal diffusivity (α) are calculated at T_f (mean film temperature of air).
- Contact resistances are neglected in the calculations.

After the heat loss calculations, the annual heat losses were calculated. Because the above-ground piping length is approximately 10 km in İzmir Geothermal Inc., heat loss values for 10 km were also checked.

Table 9. Used equations for energy analysis [48].

# of Eqn	Equation	Definition of the equation
1	$Q_{loss} = U\Delta T$	The heat loss.
2	$q = \dfrac{UA\Delta T}{L}$	The heat loss of the unit pipe length.
3	$U = \dfrac{1}{R_t}$	Overall heat transfer coefficient.
4	$R_t = \dfrac{1}{h_i * A_i} + \dfrac{\ln\left(^{r_2}/_{r_1}\right)}{2 * \pi * L * k_{steel}}$ $+ \dfrac{\ln\left(^{r_3}/_{r_2}\right)}{2 * \pi * L * k_{ins}} + \dfrac{1}{h_o * A_o}$	The total thermal resistance of the insulated pipe.
5	$\overline{Nu_D} = \dfrac{h * D}{k}$	Nusselt Number.
6	$h_i = \left(\dfrac{k_{water}}{D_i}\right) * Nu_D$	The internal heat transfer coefficient.
7	$Re = \dfrac{\rho * V * D_i}{\mu}$	Reynolds Number. If $Re > 2 * 10^5$ so flow is turbulent So, for $Re > 2 * 10^5$ Friction factor is $f = 0.184 * Re^{-\frac{1}{5}}$.

Cont. of Table 9.

8	$$Pr = \frac{Cp * \mu}{k}$$	Prandl Number.
9	$$Nu_D = \left(\frac{\frac{f}{8} * (Re - 1000) * Pr}{1 + 12.7 * \left(\frac{f}{8}\right)^{0.5} * \left(Pr^{2/3} - 1\right)} \right)$$	Nusselt correlation for internal flow. Turbulent fully developed, $0.5 \leq Pr \leq 2000$, $3000 \geq Re_D \geq 5 * 10^6, (L/D) \geq 10$.
10	$$h_o = h_{conv} + h_{rad}$$	The external surface heat transfer coefficient.
11	$$h_{conv} = \left(\frac{k_{air}}{D_o}\right) * Nu$$	The convection heat transfer coefficient over the horizontal circular cylinder surface. Thermodynamic properties of air at average temperature, T_f.
12	$$Nu = \left(0.6 + \frac{0.378 * Ra^{\frac{1}{6}}}{\left(1 + (0.559/Pr)^{\frac{9}{16}}\right)^{\frac{8}{27}}} \right)^2$$	Nusselt correlation for circular horizontal cylinders for both laminar and turbulent flow regimes.
13	$$Ra = \frac{g * \beta * (T_s - T_o) * D_o^3}{\alpha * \vartheta}$$	Rayleigh Number. Where; $\beta = {}^{1}/_{T_f}$ $T_f = \frac{T_s + T_o}{2}$
14	$$h_{rad} = \varepsilon * \sigma * \left(T_s{}^2 + T_o{}^2\right) * (T_s + T_o)$$	The radiation heat transfer coefficient. $\sigma = 5.67 * 10^{-8} \frac{W}{m^2 K^4}$
15	$$T_{os} = T_i - \left(q * R_{pipe}\right)$$	The temperature of outer surface of the pipe.

CHAPTER 5

RESULTS and DISCUSSION

As a result, a comparison between three aerogel blankets was made. In the experiment, aerogels are arranged at similar pipes, valves, and heat exchangers; the thickness and densities of aerogels should be identical for a better and optimal comparison.

Another comparison was made between two rock wool samples. Same as in the aerogel blanket experiment, the rock wool samples are arranged at similar test setup.

After all characterization studies, energy analysis and modeling were made. Results are given in this chapter.

5.1. Experimental

This section made for aerogel blankets and rock wools in order. Experimental test setup for aerogel blankets was installed in İzmir Geothermal Energy Industry Inc. B4A well. For rock wools the test setup was installed in BD11 well.

5.1.1. Aerogel Blankets

The test setup, which is prepared in İzmir Geothermal Energy Industry Inc. for aerogel blankets in the B4A well, and measurement points are given in Figure 23. Measurements were taken on 29/06/2020. Data taken from the test setup is given in Table 10. Two foreign-origin aerogel blankets are represented as A and B, and one domestic product as C.
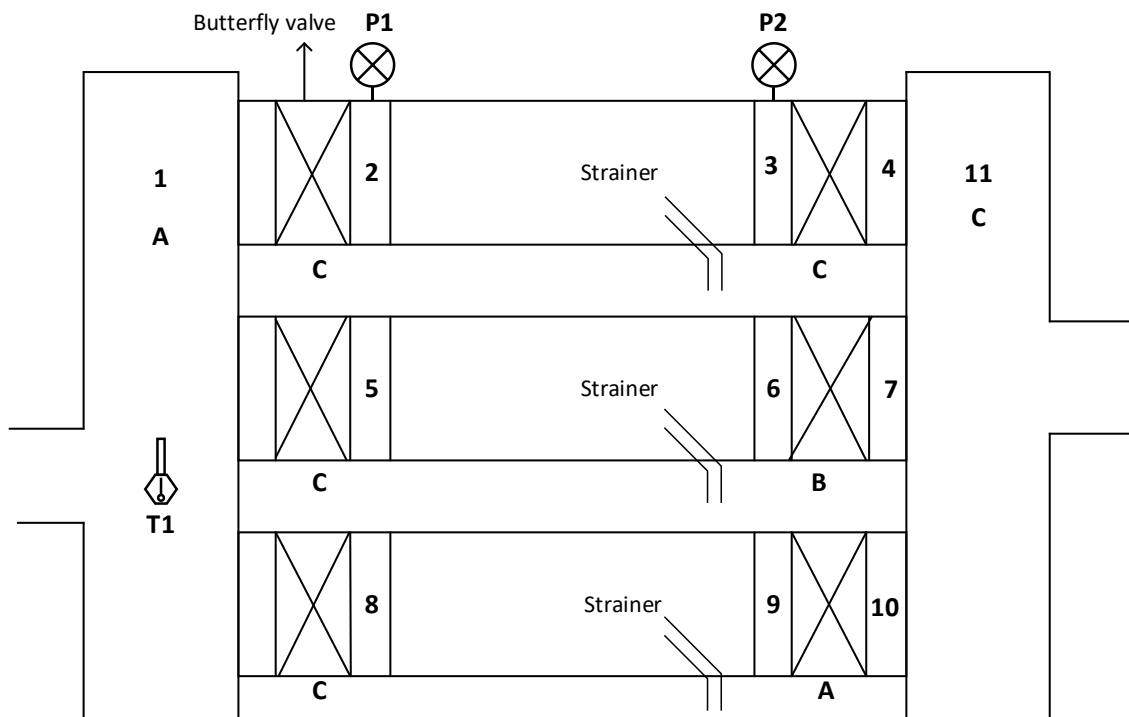
Figure 23. Schematic representation of the test setup.

Table 10. Test setup measurement data for aerogel blankets.

Measurement point	Temperature (°C)	Type of aerogel blanket
T1	102.0	Geothermal fluid temperature
1	42.8	A
2	42.8	C
3	47.7	C
4	44.2	C
5	54.5	C
6	53.3	B
7	48.3	B
8	48.0	C
9	50.3	A
10	47.6	A
11	44.7	C

Cont. of Table 10.

T$_o$	36.2	Environment temperature
Measurement point	**Pressure (bar)**	**Type of aerogel blanket**
P1	2.1	C
P2	2.2	C

As seen in Table 10, the lowest surface temperatures (44.2-47.7°C) were recorded at 3-4 points where blanket C was mounted for the same geothermal fluid inlet temperature and pressure. Blanket A and B follow C.

5.1.2. Rock wools

At 28/10/2021, the rock wool, which was used for about 8 years in the BD11 well, was removed after all temperature measurements. After installing the new rock wool, the temperature measurements were again made. The old and rock wools are from the same company, and the rock wool type is also the same. In Figure 24, the measurement points are shown in simple representation of the test setup. Test setup measurements are listed in the Table 11.
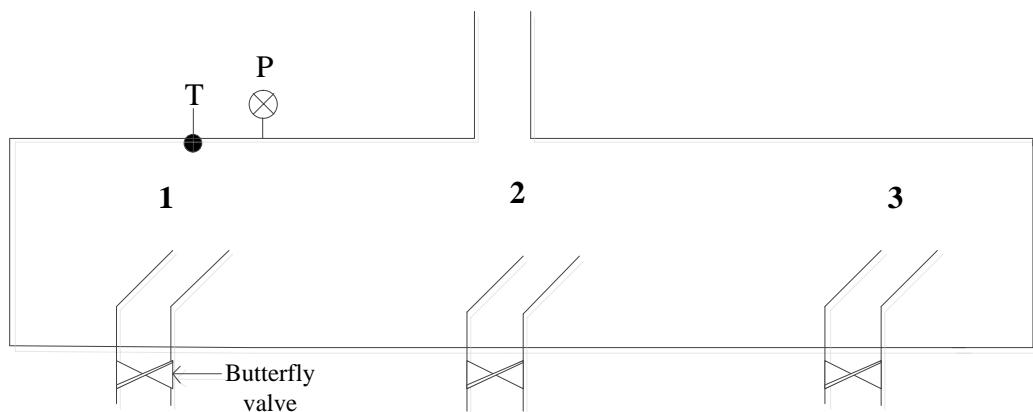
Figure 24. Drawing of test setup for rock wools.

Table 11. Test setup measurement data for rock wools.

	Measurement point	Temperature (°C)
	Geothermal Fluid	106.0
Old rock wool	1	27.7
	2	30.0
	3	30.3
New rock wool	1	27.9
	2	26.4
	3	25.5
	Environment	26.7

As seen in Table 11, the temperature measurements from the new rock wool are at a lower temperature in general.

5.2. Laboratory studies

The aerogel blankets and rock wools used in the test setup were removed from the places where they were mounted and brought to IZTECH for laboratory tests. Samples were prepared by cutting into sizes suitable for each analysis type, and aerogel samples were separated from the outer fabric coating.

5.2.1. Aerogel Blankets

The thicknesses of aerogel blankets were measured before any analysis method and are listed in the Table 12.

Table 12. The thicknesses of aerogel blankets.

Sample	A	B	C
Thickness (mm)	10	15	10

5.2.1.1. Density measurements

As a result of the measurements, it has been observed that some components in the aerogel blankets fly away and lose mass depending on the temperature. It is seen that the companies catalog data is much higher than the measured values. The blanket with the highest density is C blanket. Blanket C is followed by blankets B and A, respectively. Blanket B is 5 mm thicker than other blankets. This can be a disadvantage in terms of cost and usage. Table 13 shows the different temperatures and the densities of aerogel blankets at these temperatures.

Table 13. Densities of aerogel blankets at different temperatures.

Temperature (°C)	Density (kg/m^3)		
	A	B	C
30	164 ± 0.135	181 ± 0.148	192 ± 0.159
110	162 ± 0.133	178 ± 0.146	191 ± 0.159
765	156	170	184

5.2.1.2. Thermo gravimetric analysis (TGA)

As a result of TGA analysis, the mass loss caused by burning the aerogel blankets at 765°C is about 5% for the A blanket, about 6% for the B blanket, and about 4% for the C blanket. TGA analysis graphs are shown in Figures 25-26.

Total weight loss can be attributed to three different phenomena. The loss of physical water up to 100°C, first part concerns physical water evaporation, the second part was due to residual organic solvents evaporation at temperatures ranging from 100 to 240°C. Usually, this part can be neglected. The last part corresponds to the loss due to the oxidation of Si–CH$_3$ groups on the aerogel surface and the oxidation of the methyl groups. These results showed that the blanket was stable up to 650°C. It can be attributed to the presence of fiberglass in the blanket [49]. Aerogels contain some binders that dissociate upon the first heating of the insulation blanket material. Because the maximum

expected service temperature of these blankets is less than 200°C, the thermal stability of aerogel blankets should not be an issue.
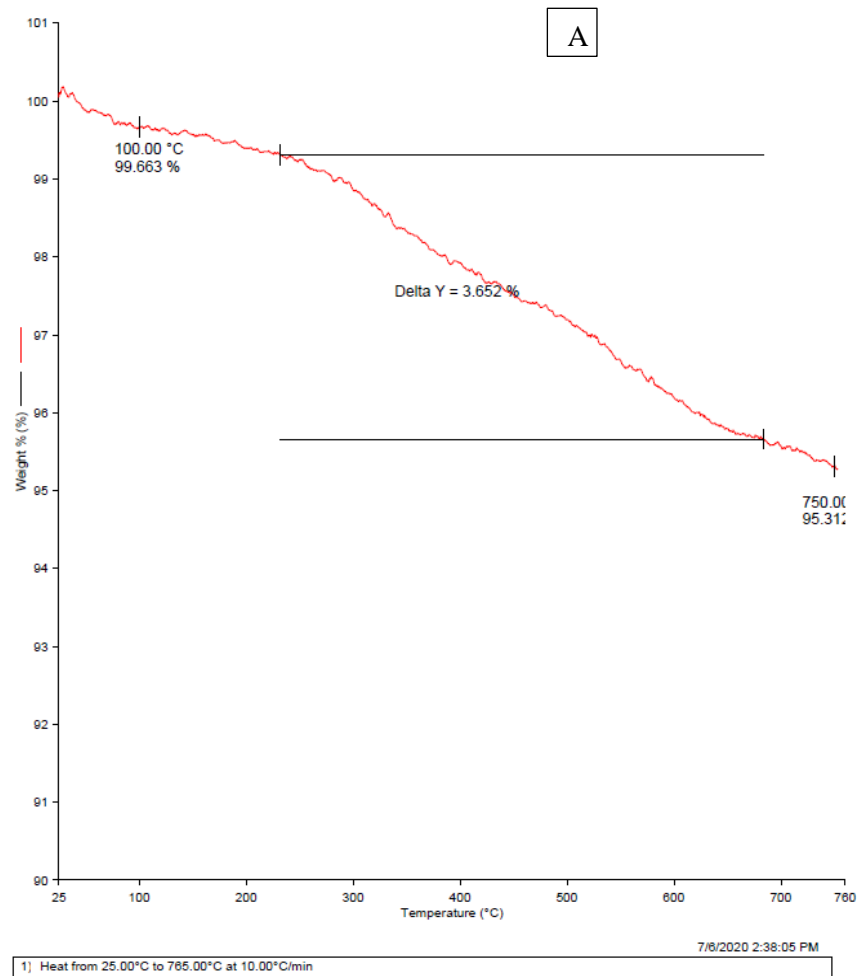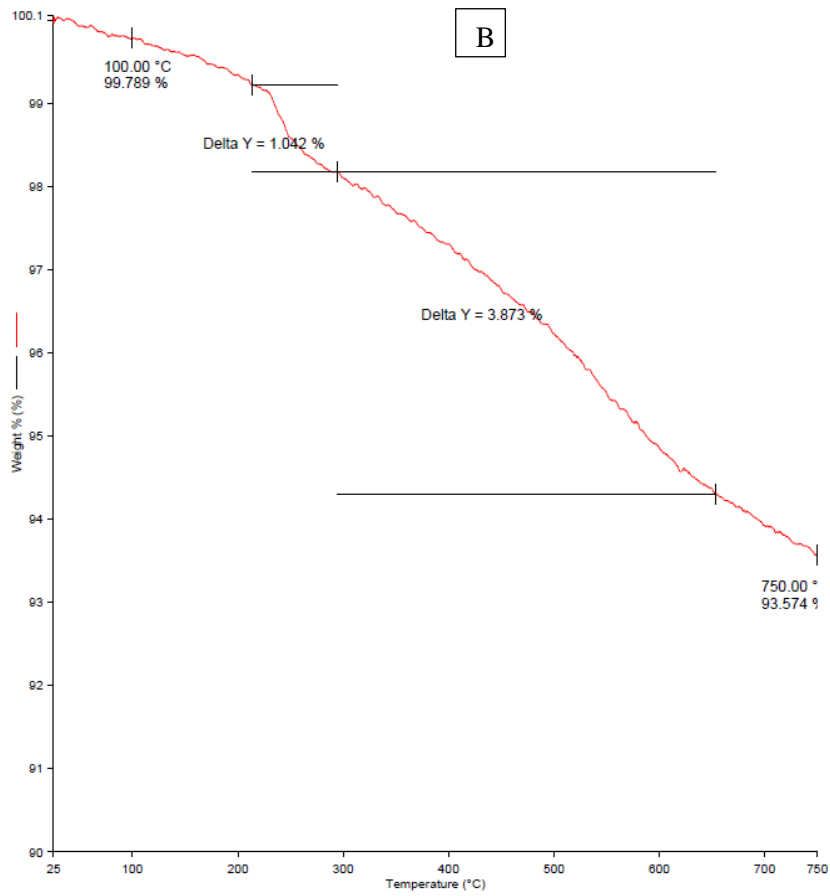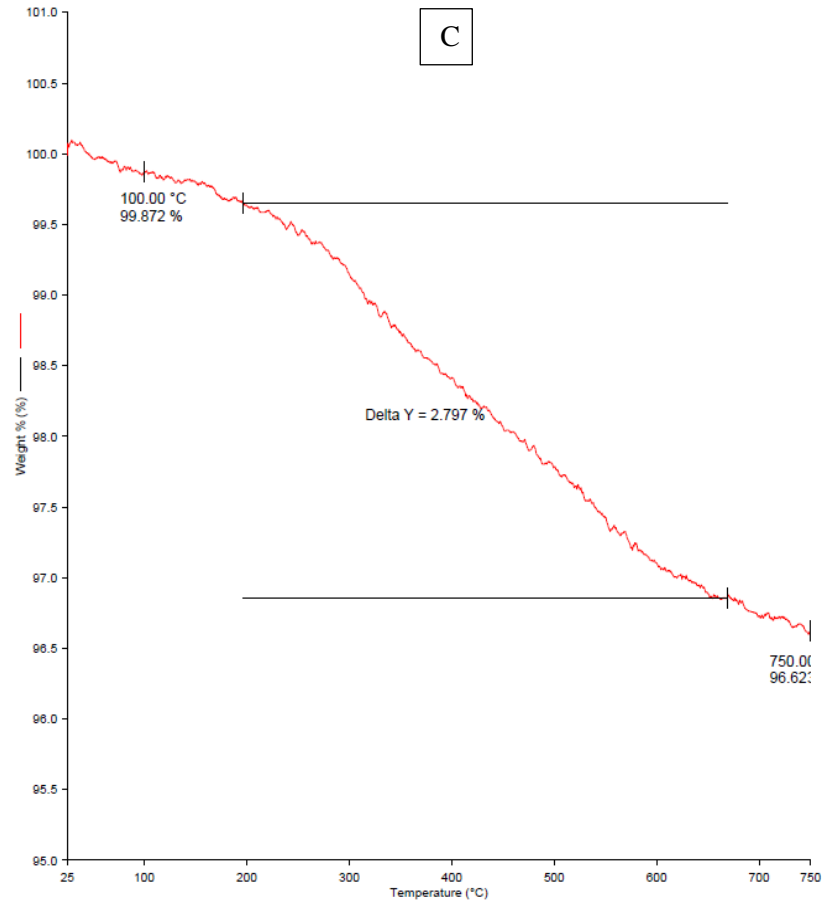

Figure 25. TGA plots of aerogel blanket type A.

Figure 26. TGA plots of aerogel blankets type B and C.

5.2.1.3. Optical microscope images

The sample images observed at approximately 40x magnification with an optical microscope, it was observed that all three samples had a fiber-like shape. Stereo zoom optical microscope images of the samples are shown in Figure 27.
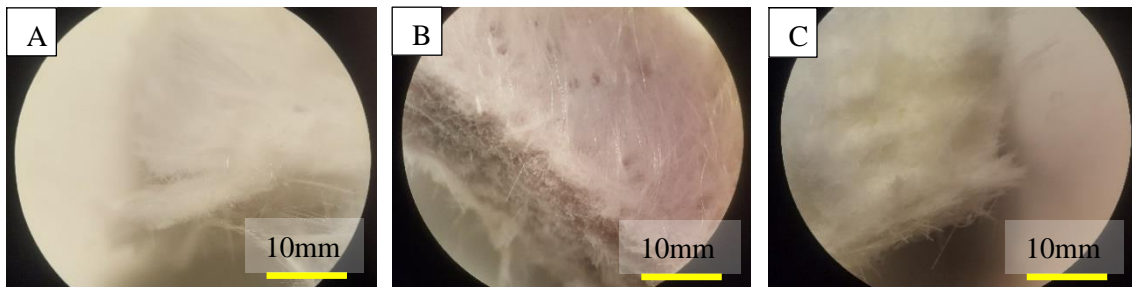

Figure 27. Stereo Zoom Optical microscope images of aerogel blankets, respectively.

5.2.1.4. Scanning electron microscopy (SEM) observations

As a result of SEM images, it was observed that the aerogels were in the form of coaxial particles and attached to some silicate fibers (glass fibers) in all three samples. Considering that the aerogel particles are airborne due to their small size, it is thought that each insulation blanket is manufactured by being impregnated on the fiber structure during its manufacture.

However, it should be taken into account that the aerogel particles may spill over the glass fibers on which they are attached during the sample preparation process. The SEM images showed that the blanket with the strongest adhesion of the aerogel particles to the fibers belonged to the C sample and the weakest to the A sample. It was also observed that in sample C, the dimensions of the aerogel particles were more significant than those of the other two aerogel blankets. It is a useful feature in terms of continuity of performance. Due to the high adhesion in sample C is likely to measure lower surface temperature than blanket B. In addition, due to this feature, it is thought that the performance loss of the C blanket will be lower depending on time. Figure 28 shows SEM images of all three aerogel blankets at 250x magnification, and Figure 29 shows SEM images at 50000 x magnifications.
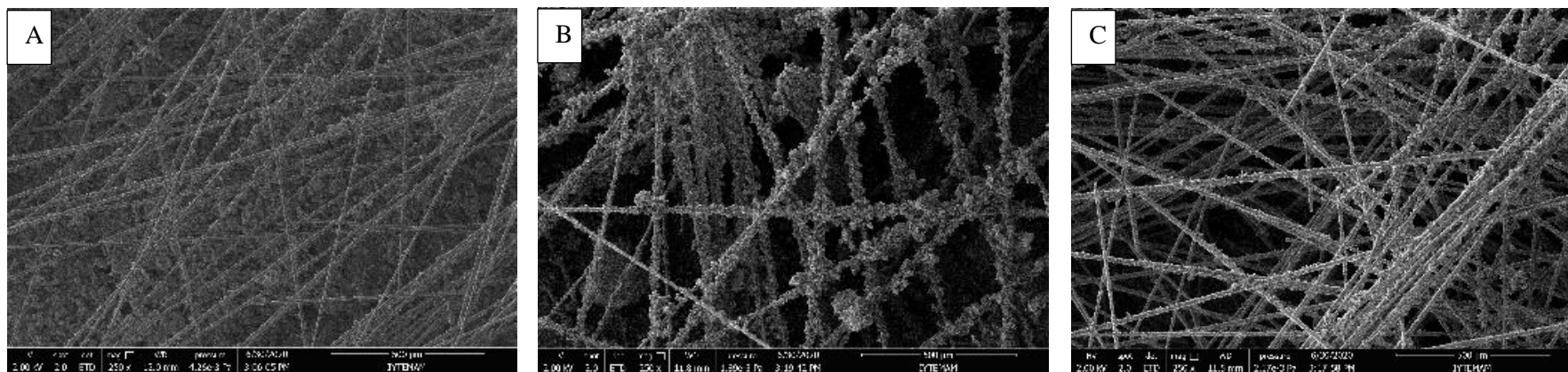
Figure 28. SEM images of aerogel blankets at 250x magnification, respectively.
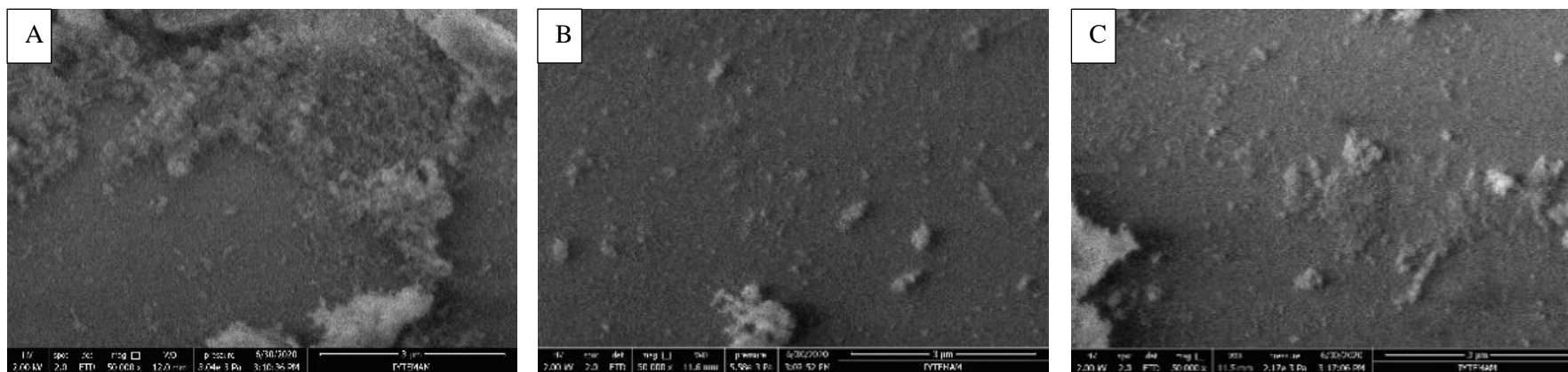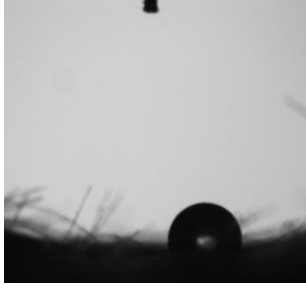
Figure 29. SEM images of aerogel blankets at 50000x magnification, respectively.

5.2.1.5. Contact angle measurements
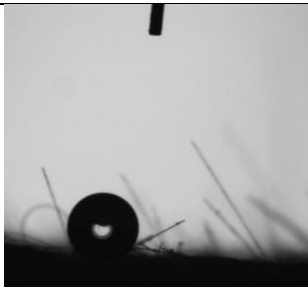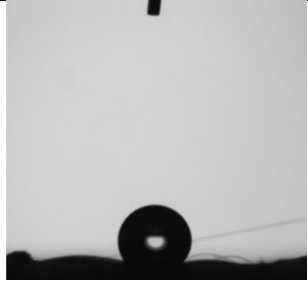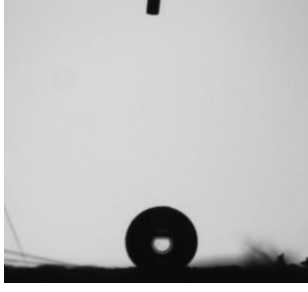
Aerogel blanket manufacturers have declared that all three products exhibit non-wetting properties. As a result of the contact angle measurements, it is seen that A aerogel blanket has the best non-wetting property compared to other blankets, followed by C and B. Although it was stated that the same fabric was used for all aerogel blankets as a cover, separate measurements were made because color differences were observed. Since the cover material protects the aerogel blanket from the external environment, the contact angle measurement is considered more important than the blanket. With the cover measurements, the contact angle is B, C, and A from high to low. The obtained contact angle data are in a good agreement with the literature [26, 36]. In Table 14, the measured contact angles and contact angle measurement images of all three aerogel blankets; with and without covering material are listed in order.

Table 14. Contact angle measurements and images for aerogel blankets.

Sample	Measured contact angle (°)	Images of contact angles
A	146 ± 2.36	
B	100 ± 1.17	

Cont. of Table 14.

C	125 ± 1.17	
A – covered	127 ± 1.04	
B – covered	145 ± 2.65	
C – covered	129 ± 2	

5.2.1.6. Energy dispersive X-ray (EDX) observations

When the three aerogel blankets are compared to each other, each blanket has common elements of carbon, oxygen, aluminum, silicon, and calcium; unlike the others, some magnesium was detected in the C aerogel blanket. The possible reason for this was considered to be the chemicals used in the aerogel synthesis. In addition, the high amount of carbon in blanket A indicates that there is SiC in the content. It has been evaluated that this is due to the aerogel synthesis approaches. For aerogel blanket A; Spectrum 3 is fiber, Spectrum 4 is aerogel. For aerogel blanket B; Spectrum 1 is fiber, Spectrum 2 is aerogel.

For aerogel blanket C; Spectrum 5 is fiber, Spectrum 6 is aerogel. Figures 30-32 shows the regions of EDX measurements of A, B, and C aerogel blanket samples, respectively. Table 15 shows the chemical analysis of aerogel blanket samples in EDX elemental form, whereas Table 16 shows the chemical analysis of aerogel blanket samples in EDX oxide form.
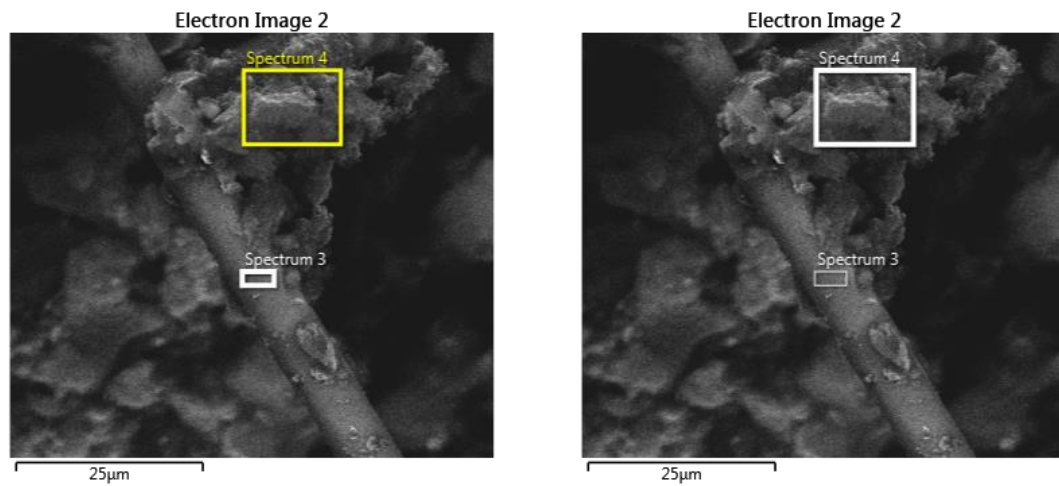
Figure 30. The region of the EDX measurement was taken from the aerogel blanket sample of A.
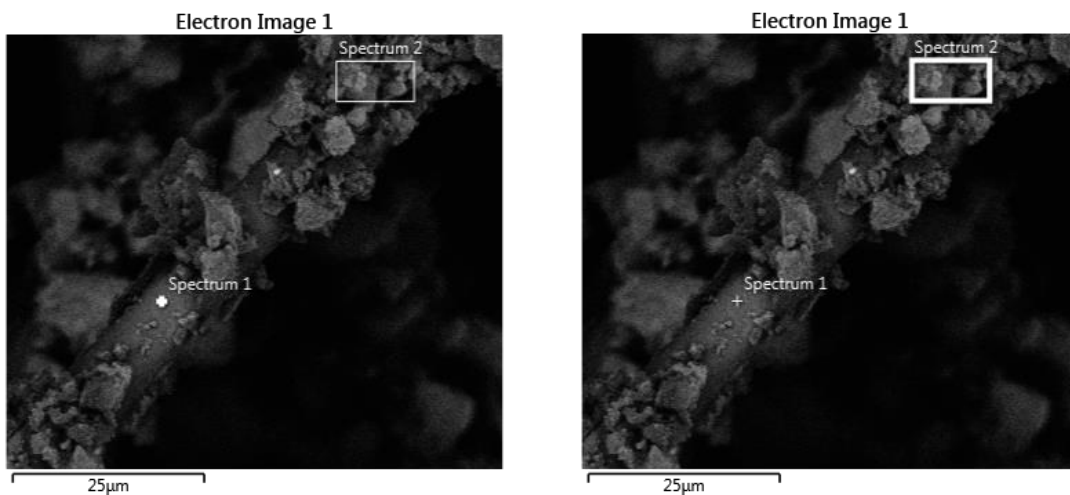
Figure 31. The region of the EDX measurement was taken from the aerogel blanket sample of B.
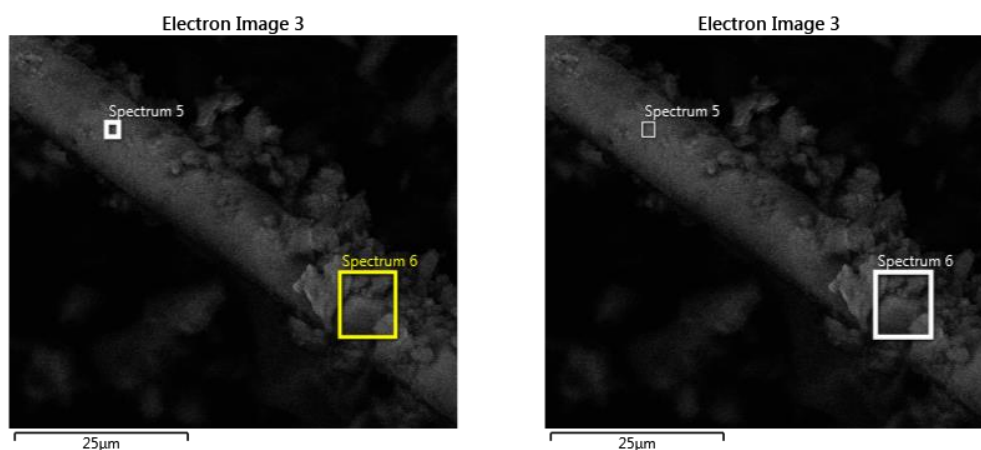
Figure 32. The region of the EDX measurement was taken from the aerogel blanket sample of C.

Table 15. Chemical analysis of aerogel blanket samples in EDX elemental form.

Weight (%)						
The element	A – aerogel	B – aerogel	C – aerogel	A – fiber	B – fiber	C – fiber
C	15.80	11.80	4.89	6.01	7.63	8.18
O	53.03	51.47	57.63	50.55	59.78	55.70
Al	0.79	4.10	5.16	5.04	3.73	3.74
Si	29.39	24.27	21.68	26.85	22.04	22.46
Ca	0.98	8.36	9.02	11.56	6.82	8.66
Mg	-	-	1.62	-	-	1.27
Total	100	100	100	100	100	100

Table 16. Chemical analysis of aerogel blanket samples in EDX oxide form.

Oxide weight (%)						
Oxide	A – aerogel	B – aerogel	C – aerogel	A – fiber	B – fiber	C – fiber
Al_2O_3	1.79	12.15	10.28	11.45	11.06	14.18
SiO_2	75.63	81.46	69.89	69.09	73.97	67.46
CaO	1.65	18.35	17.62	19.45	14.97	18.36
MgO	-	-	1.85	-	-	2.36
Total	79.07	111.96	97.79	100	100	100

5.2.1.7. Thermal conductivity analyses

In Table 17, the thermal conductivity measurements are tabulated. As seen in from the table, sample B has the lowest thermal conductivity as both blanket and blanket+cover. While the A sample is in the 2nd place in the thermal conductivity as a blanket, it is in the 3rd place as the blanket+cover. While C is in the 3rd place after A in blanket measurements, it is in the 2nd place in blanket+cover. When the cover is added, the thermal conductivities increase due to the higher thermal conductivity of the cover material. When the C sample is considered as blanket+cover, it is seen that it has a thermal conductivity close to the B blanket. However, this still does not explain the lower surface temperature of the C blanket.

Table 17. The thermal conductivity measurements for aerogel blankets, and the cover material.

Sample	k (W/mK)	T_m (°C)	Density (kg/m³)	Firm declaration at 25°C λ (W/mK)
A	0.0312	28	162	0.024
B	0.0278	35	178	0.021
C	0.033	29	191	0.0136
A – Cover	0.05	32	-	-
B – Cover	0.042	32	-	-
C – Cover	0.0433	32	-	-

5.2.1.8. X-ray diffractometry (XRD) observations

In line with these analyses, it was observed that all of the aerogel blanket samples were in an amorphous structure, and this observation proves that the fibers in the company catalogs are glass fibers. The peak around the angle of 23 proves the amorphous and nanostructure of the aerogels. Other peaks with smaller intensities shown in blanket B

could be due to additional silica peaks. Figure 33 shows XRD plots of aerogel blankets, A, B, and C, respectively.
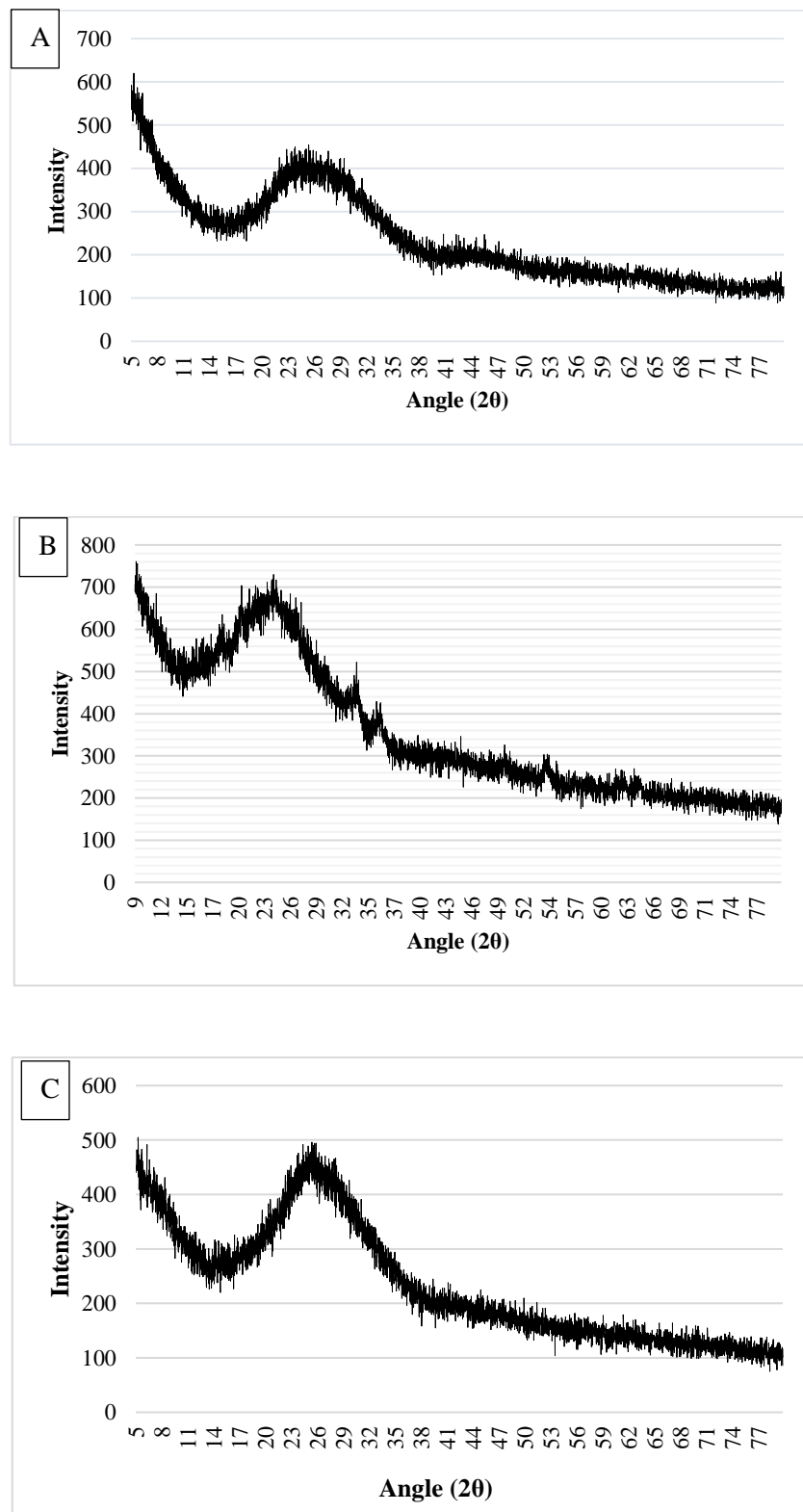
Figure 33. XRD plots of aerogel blankets.

5.2.1.9. Fourier transform infrared spectrometry (FTIR) observations

As a result of the analysis, it was observed that each sample peaked at approximately 1090 cm^{-1} wave number. This peak indicates that the aerogel blankets have Si-O-Si bonding. Standard deviations for this peak are 0, 4.2, and 2.8, respectively. Again, it was observed that each sample made another peak at around 810 cm^{-1} wave number. This peak means that the aerogel blankets have Si-C bonding. Standard deviations for this peak are 1.4, 0, and 11.3, respectively. The graphs' constant permeability percentage from the wavenumber of 1360 cm^{-1} proves that the aerogel blanket samples show non-wetting properties [45]. Graphs of FTIR observations are given in Figure 34.
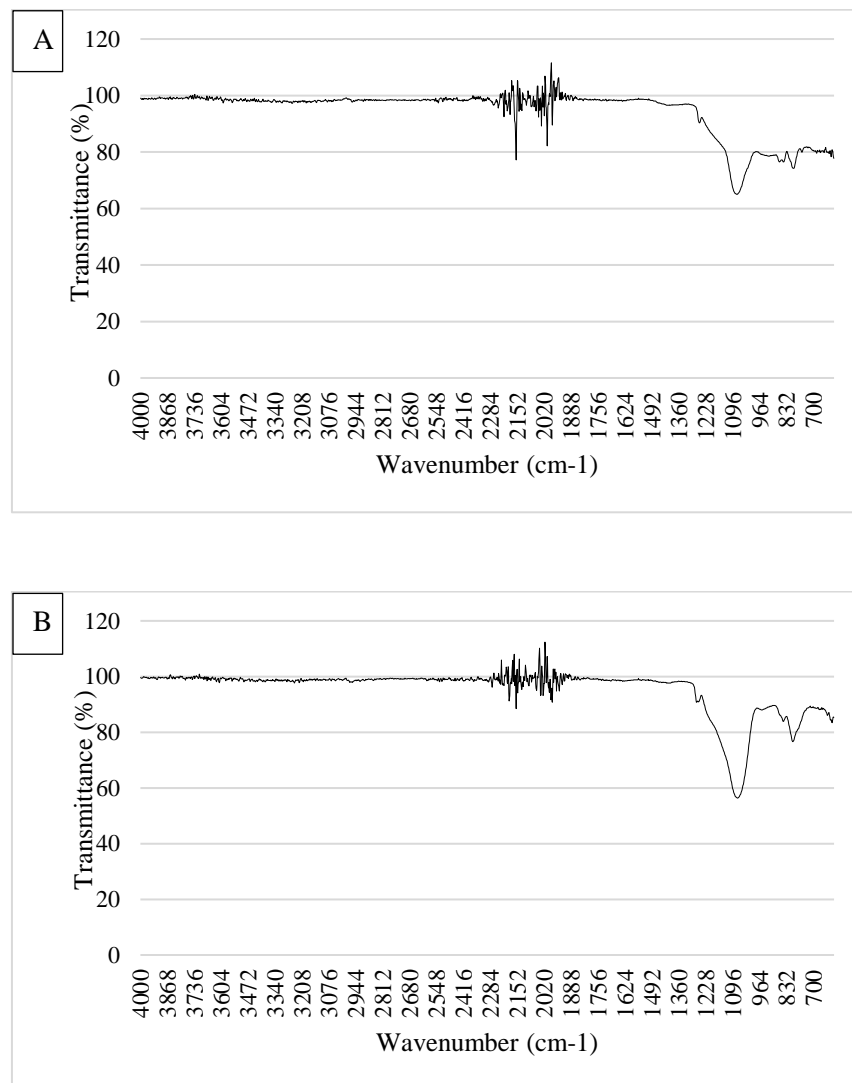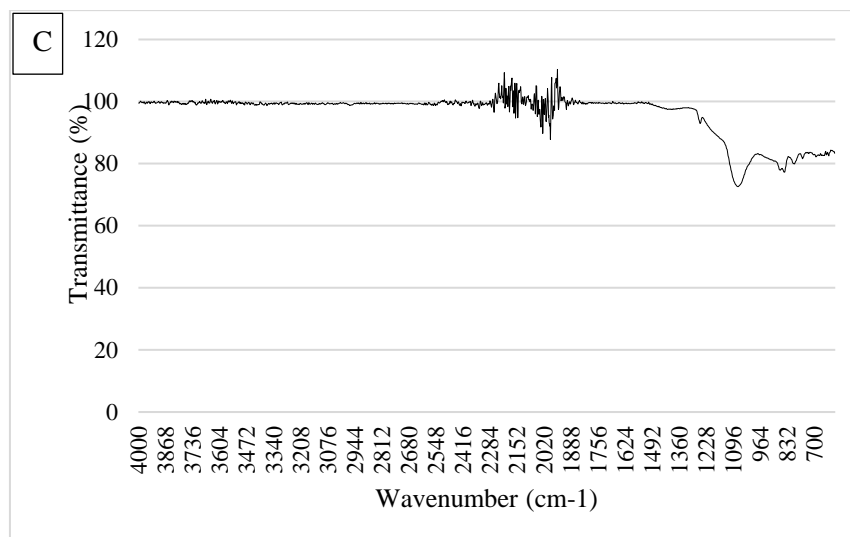
Figure 34. FTIR plots of aerogel blankets, respectively.

5.2.1.10. Heat capacity (specific heat) measurements

The heat capacity-temperature variation of aerogel blanket samples is given in Figure 35. The measured heat capacity values given in Table 18 are compatible with the literature. The highest heat capacity value at 110°C belongs to blanket C (1.5 J/gK). Blanket C is followed by blanket B (1.36 J/gK) and blanket A (1.16 J/gK). The fact that the C blanket's surface temperature is lower, the heat capacity is higher than the other blankets. The large heat capacity slows down the heat transfer and is preferred for insulation purposes.

Table 18. The specific heat capacity measurements of aerogel blankets at 110°C.

Temperature (°C)	Sample	Heat capacity (C_p) (J/gK)
110	A	1.19 ± 0.33
	B	1.36 ± 0.36
	C	1.50 ± 0.2
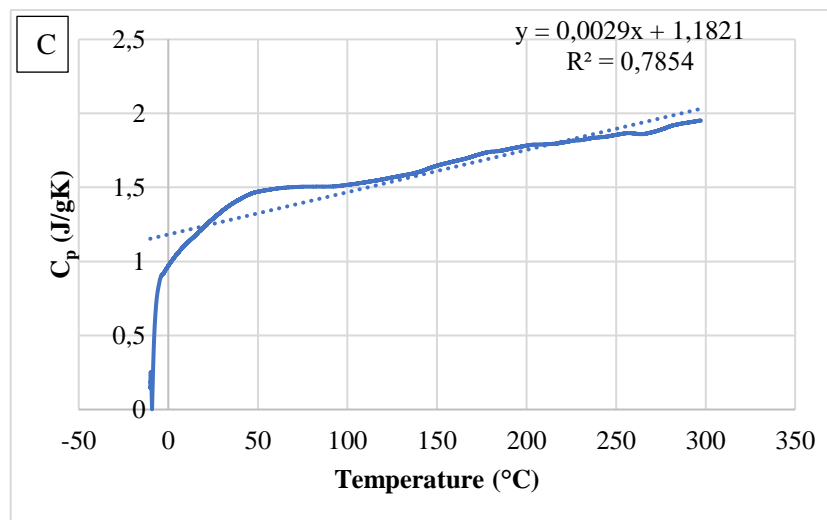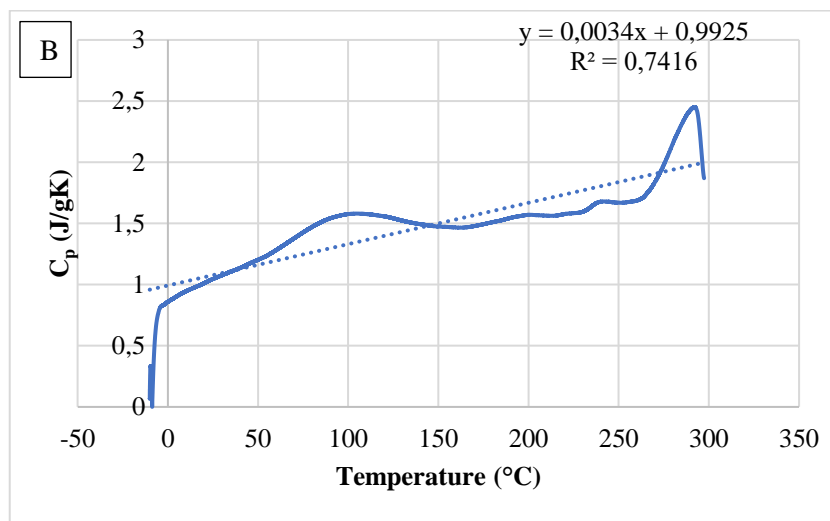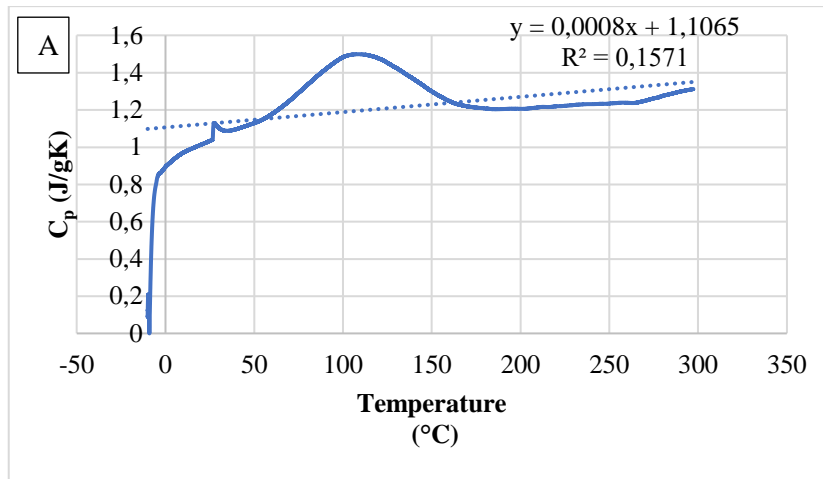
Figure 35. Heat capacity-temperature variation of aerogel blanket samples determined by DSC, respectively.

5.2.2. Rock wools

The old and new rock wool samples were taken from the test setup and brought to IZTECH for laboratory tests. Samples were prepared by cutting into sizes suitable for each analysis type. The raw thicknesses of the samples were measured and listed in Table 19.

Table 19. The thicknesses of rock wools.

Sample	Thickness (mm)
Old	100
New	100

5.2.2.1. Density measurements

In Table 20, the density values given that are calculated at room temperature, after the oven temperature of 110°C, and after TGA.

Table 20. Calculated density values of rock wool samples depending on temperature.

Temperature (°C)	Density (ρ) (kg/m^3)	
	Old	New
25	92.9 ± 0.814	124.4 ± 1.09
110	92.5 ± 0.811	124.2 ± 1.089
765	89.2	121.9

Table 20 shows that some components in rock wool fly away and lose mass depending on the temperature. According to the Izocam catalog, the density of rock wool is between 30-200 kg/m^3 [50].

5.2.2.2. Thermo gravimetric analysis (TGA)

As a result of these processes, the mass loss caused by the burning of rock wool at 765°C is approximately 4% for old rock wool and 2% for new rock wool. Respectively, Figure 36 shows the TGA plot of the old rock wool and the new rock wool, respectively.
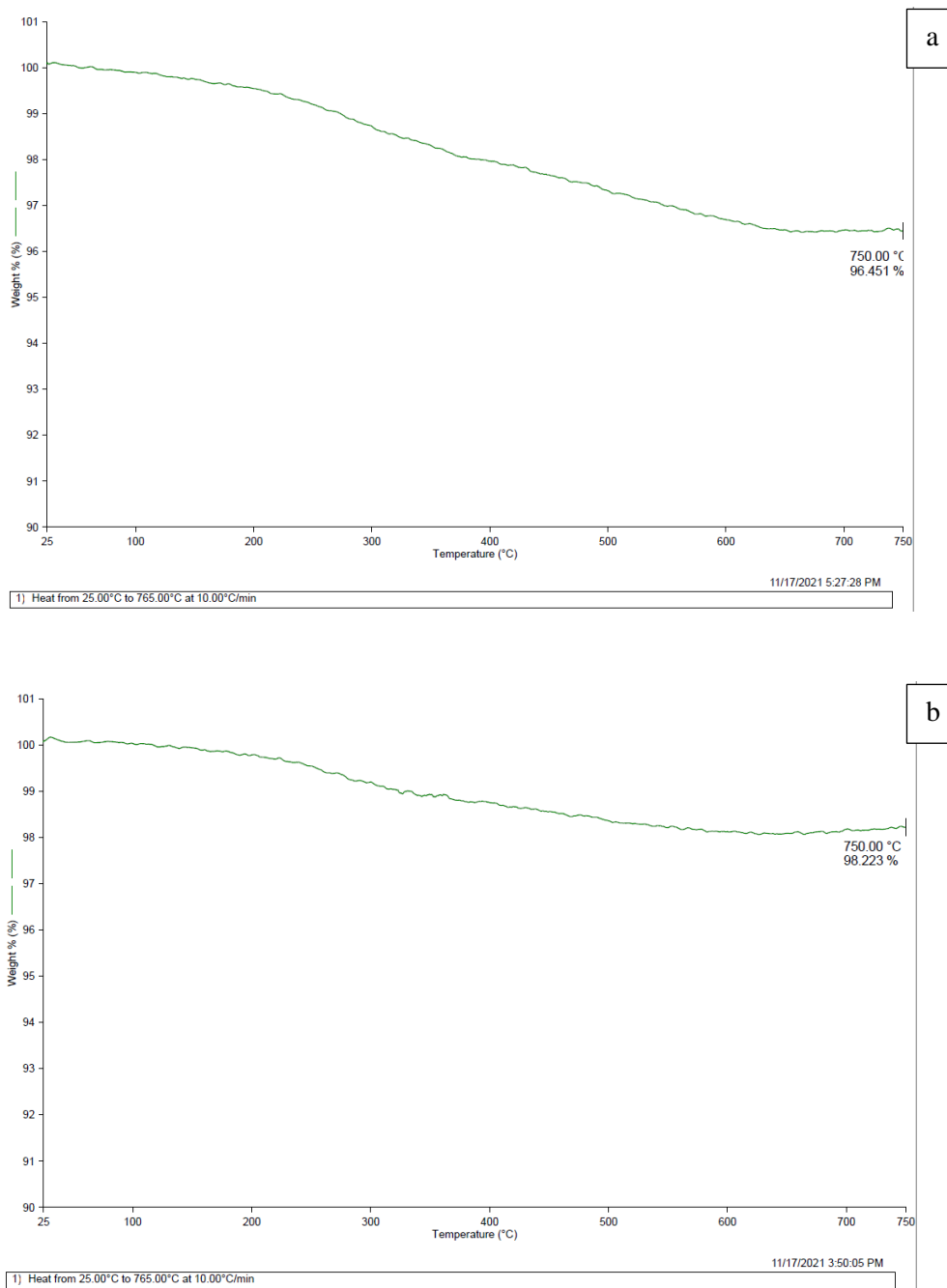
Figure 36. TGA graphs of old rock wool (a) and the new rock wool (b).

5.2.2.3. Optical microscope images

Both rock wool samples were viewed under a stereo zoom optical microscope. Sample images observed with an optical microscope were also photographed, and the images are given in Figure 37. It was observed that both samples had a fiber fibrous shape. The samples were also observed with Scanning Electron Microscope (SEM) for a more detailed observation of these fibers. Since more detailed observations are made in the electron microscope images in the next section, the scale bar is not included in the figures.
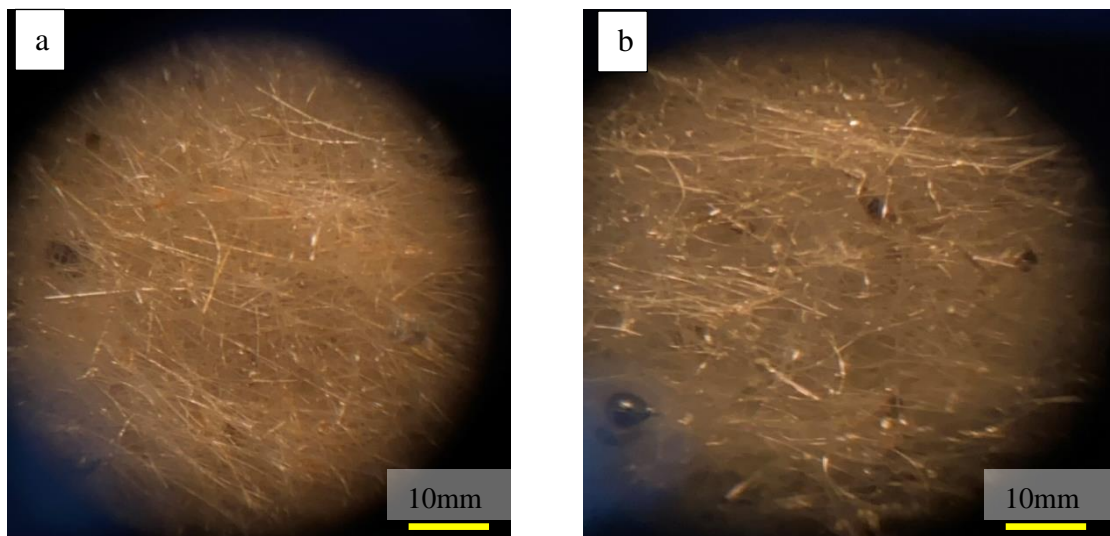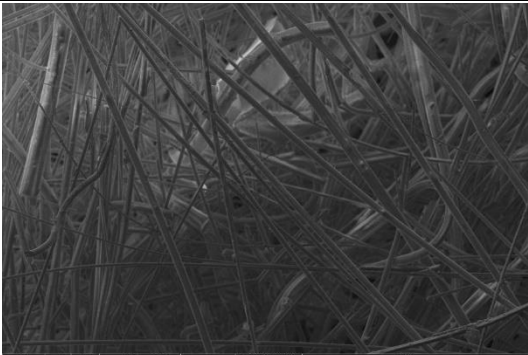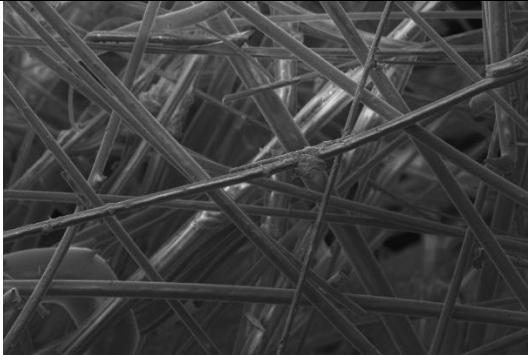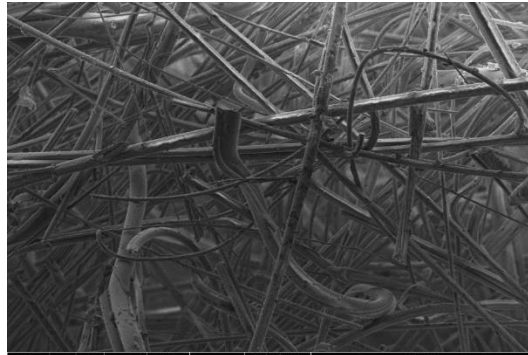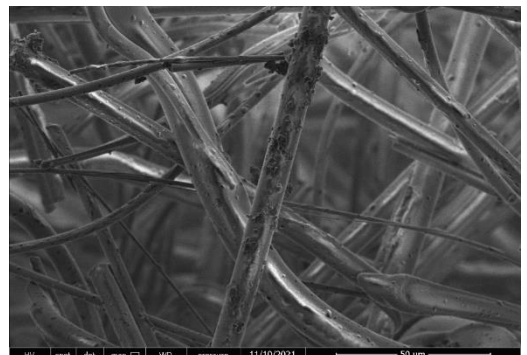
Figure 37. Stereo Zoom Optical microscope specimen images: (a) old rock wool, (b) new rock wool.

5.2.2.4. Scanning electron microscopy (SEM) observations

The images of the samples observed in the secondary electron (SE) mode at different magnifications are given in Table 21. As a result of SEM images, it was observed that rock wools are in silicate fiber (glass fiber) form.

Table 21. SEM images of rock wools at different magnifications.
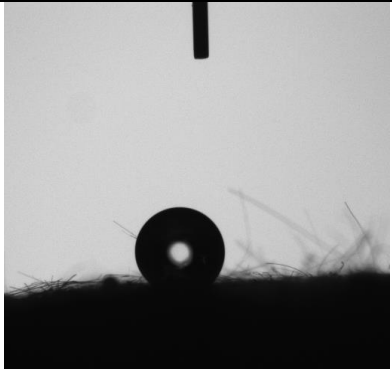
	500x magnification	1000x magnification	2500x magnification
Old			
New			

5.2.2.5. Contact angle measurements

The results given in Table 22 were obtained. Rock wool producer company has declared that the product does not have a non-wetting feature.

For a material to show instant non-wetting properties, the contact angle is expected to be greater than 90°. To measure the actual non-wetting properties of rock wool, it must be exposed to a large amount of liquid for a long time.

Table 22. Contact angle measurement results of rock wool samples.

Sample	Measured contact angle (°)	Images of contact angle
Old	134 ± 17	
New	147 ± 15	

As a result of these measurements, it is seen that the new rock wool has a better non-wetting property than the old rock wool.

5.2.2.6. Energy dispersive X-ray (EDX) observations

Figure 38 show the sample area for EDX analysis. Since it is thought that it would be more accurate to consider the oxide forms of the elements during the interpretation of the EDX results, the analysis results are listed in two tables. EDX analysis results of all samples are given in Tables 23 and 24.
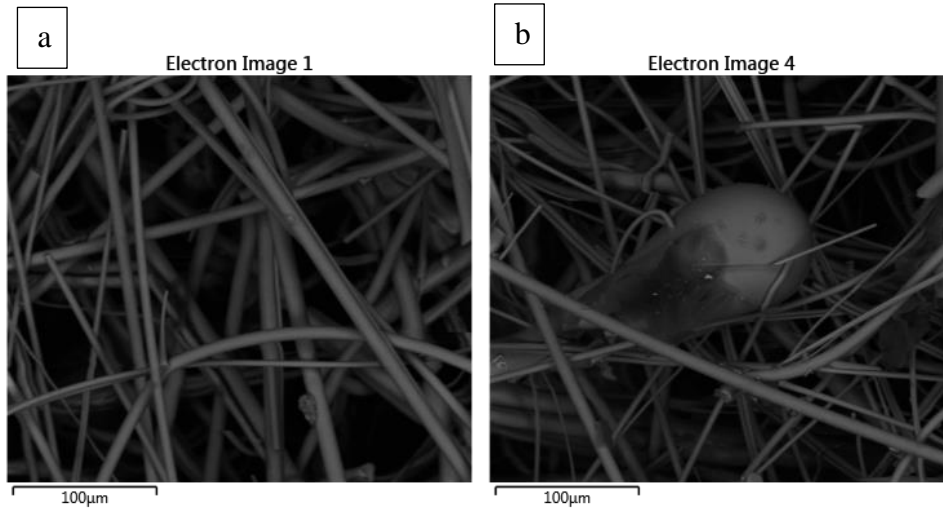
Figure 38. The region of the EDX measurement was taken from the old rock wool sample (a) and, the new rock wool sample (b).

Table 23. Chemical analysis of rock wool samples in EDX elemental form.

The element	Weight (%)	
	Old	New
C	11.00	17.84
O	42.17	39.61
Na	3.30	2.90
Mg	2.62	2.52
Al	0.54	0.64
Si	19.57	16.73
K	-	0.21
Ca	13.11	12.29
Fe	7.68	7.25
Total	100	100

Table 24. Chemical analysis of rock wool samples in EDX oxide form.

Oxide	Oxide weight (%)	
	Old	New
Na_2O	5.49	5.36
MgO	5.36	5.73
Al_2O_3	1.26	1.66
SiO_2	51.69	49.09
K_2O	-	0.35
CaO	22.65	23.59
Fe_2O_3	13.56	14.22
Total	100	100

When the two rock wools are compared, some potassium was detected in the new rock wool, different from the old one. It can be thought that the possible reason for this is that it was produced in different periods despite the rock wool production stage and the production of the same company. The iron contained in the rock wool causes the color of the rock wool to resemble green.

When the EDX analysis results are examined, it is seen that the amount of SiO_2 constitutes approximately 50% of the rock wool. This does not directly coincide with the amount of glass fiber that the rock wool company has declared as 92-96% in the MSDS document [51].

5.2.2.7.   Thermal conductivity analyses

In Table 25, the company's catalog data [10] and measured data are listed. The thermal conductivity is indicated by k (W/mK).

Table 25. Measured thermal conductivities and catalog data of rock wool samples.

Sample	k (W/mK)	Tm (°C)	Density (kg/m³)
Old	0.0393	31	92.9
New	0.0348	32	124.4
Catalog [9]	0.038	50	30-200
	0.047	100	

The new rock wool sample has a lower thermal conductivity coefficient. Although the catalog temperature and the measurement temperature are not equal, the thermal conductivity overlaps.

5.2.2.8. X-ray diffractometry (XRD) observations

Analyses were made for both rock wool samples, and the graphs created as a result of the analysis are given in Figure 39. The XRD analyses showed that both samples were amorphous.
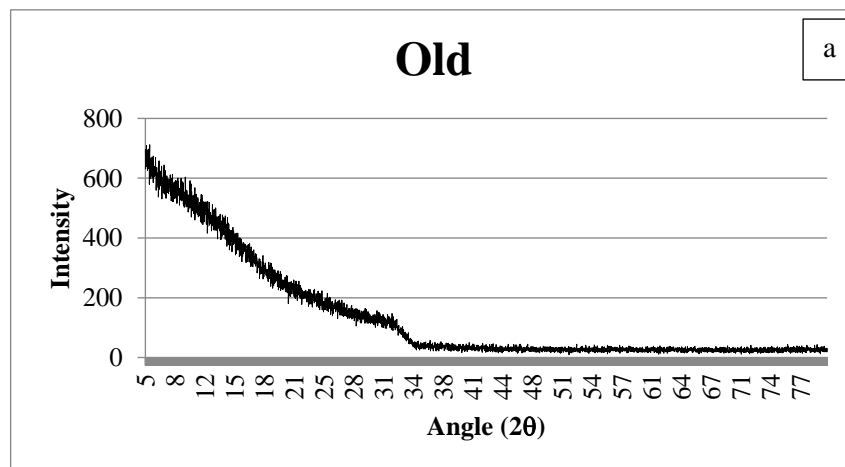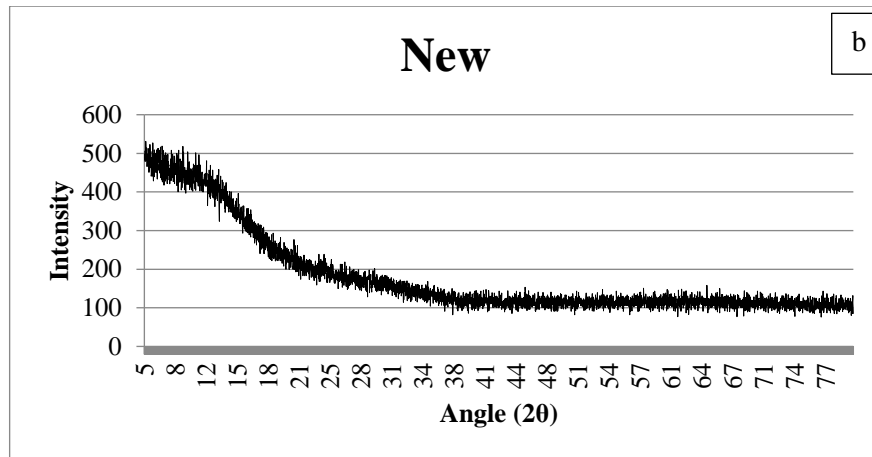
Figure 39. XRD analysis graphs of rock wool samples: (a) old, (b) new.

5.2.2.9. Fourier transform infrared spectrometry (FTIR) observations

FTIR spectrometer analysis graphs of each rock wool sample are given in Figure 40. In the light of these graphs, it was observed that each sample peaked at approximately 860 cm^{-1} wave number. This peak shows that stone wools have Si-O-Si bonds.

The peaks seen between 1800 and 2240 cm^{-1} in each graph are due to a systematic error caused by the device and should not be taken into account. Standard deviations for old and new rock wool calculated as 13.6 and 9.
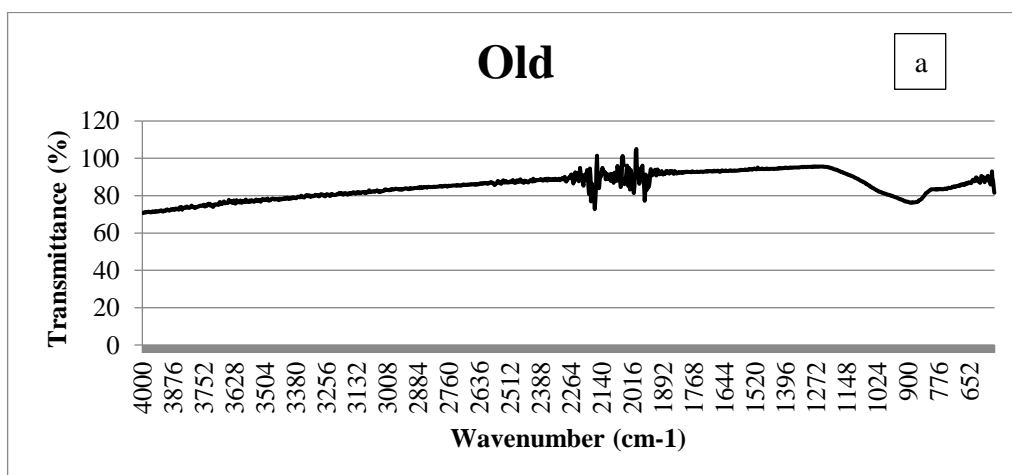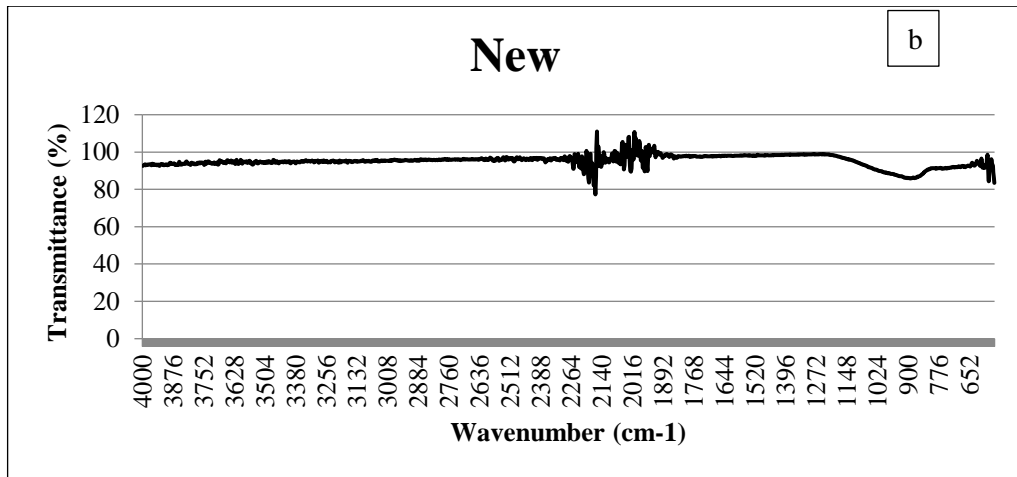
Figure 40. FTIR analysis graphs of rock wool samples: (a) old, (b) new.

5.2.2.10. Heat capacity (specific heat) measurements

The heat capacity calculations were made by using the slope of the determined heat capacity versus temperature graphs which are evaluated after DSC measurements, given in Figure 41 for both the old and the new rock wools, respectively.
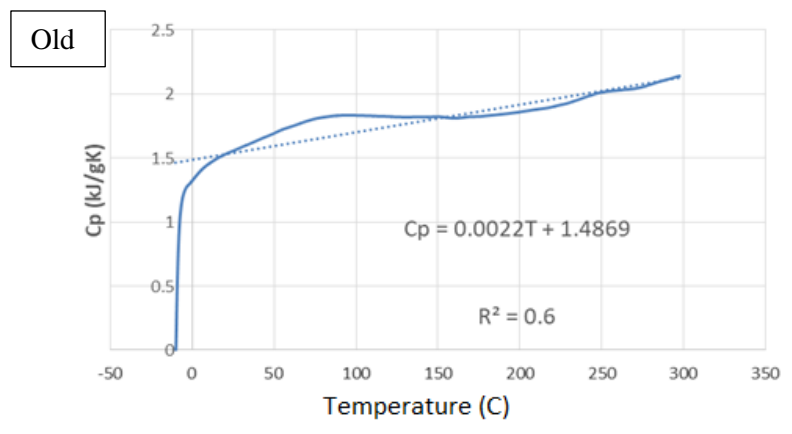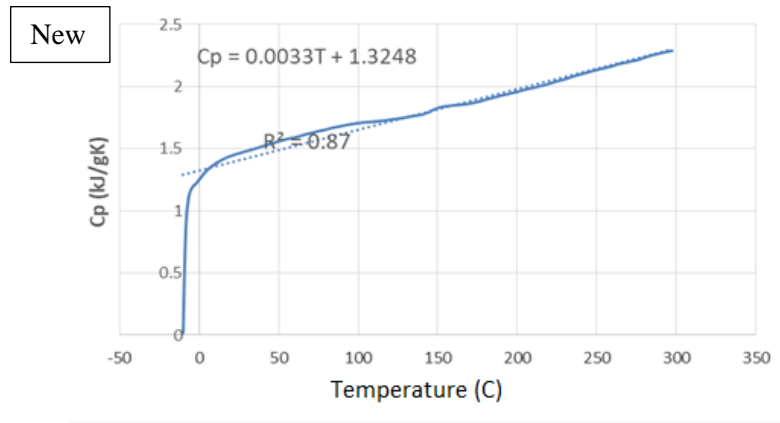
Figure 41. DSC-determined heat capacity-temperature variation of rock wool samples: old, new.

The heat capacity values were calculated for 110°C representing the average geothermal operating temperature, which is one of the temperatures we used in the density calculation given in Table 26. Standard deviations for old and new rock wool as 0.27 and 0.36. Values are in agreement with the literature.

Thermal conductivity and heat capacity are inversely proportional. Since rock wool is used for insulation purposes, it is preferable to have a large heat capacity. According to Table 26, the heat capacity value of the old rock wool sample at 110°C is higher than the heat capacity value of the new rock wool.

Table 26. Heat capacity values of stone wool samples were calculated at 110°C.

Temperature (°C)	Sample	Heat capacity (C_p) (J/gK)
110	Old	1.73 ± 0.27
	New	1.69 ± 0.36

5.3. Energy Analysis

Energy analysis was conducted to obtain the amount of heat loss for unit pipe length for each aerogel blanket and rock wool insulation materials. Since the heat loss is related to the total thermal resistance and overall heat transfer coefficient, firstly, the internal and external convective heat transfer coefficients were calculated. Then, the overall heat transfer coefficient, thermal resistance, and finally, the heat loss values were calculated. T_s are the temperatures of the surfaces of insulation materials that were measured in the experiment section.

This thesis focuses on suitable material selection. Using the right insulation material decreases heat losses; this section examines the heat losses for the established test setup for aerogel blankets and rock wools.

5.3.1. Aerogel Blankets

The collected data from the setup are used to calculate the heat transfer coefficients and heat loss per unit length for bare pipe and each aerogel blankets. The blankets A and C have the same thickness as 10 mm while the thickness of blanket B is 15 mm. To be able to evaluate all blankets under the same condition, all parameters for blanket B are also calculated for a thickness of 10 mm. Another case was evaluated without insulation material to make a complete comparison study. All calculated heat loss parameters and the heat loss values are listed in Table 27.

Table 27. Energy analysis results for aerogel blankets.

	A (10 mm)	B (15 mm)	B (10 mm)	C (10 mm)	Bare pipe without insulation
k_{ins} [W/mK]	0.0312	0.0278	0.0278	0.033	
k_{cover} [W/mK]	0.05	0.042	0.042	0.0433	-

Cont. of Table 27.

r_3 [m]	0.09415	0.09915	0.09415	0.09415	-
r_4 [m]	0.09615	0.1012	0.09615	0.09615	
T_s [K]	322.1	324	340.1	319.1	375.1
h_i [W/m^{2}K]	1846	1846	1846	1846	1846
h_{conv} [W/m^{2}K]	0.09781	0.0953	0.1057	0.0956	0.1229
h_{rad} [W/m^{2}K]	6.784	6.844	7.394	6.686	5.413
h_o [W/m^{2}K]	6.882	6.94	7.5	6.782	5.536
U [W/m^{2}K]	1.128	0.8534	1.15	1.262	2.915
R_t [m^{2}K/W]	0.8867	1.172	0.8696	0.7922	0.3431
q [W/m]	43.9	34.98	44.76	49.14	101.4

As expected, the cold-drawn steel pipe without any insulation tends to have the highest heat loss. The aerogel blanket B (15 mm) shows lower heat loss than aerogel blanket B (10 mm) with a 25.8 %. If the thicknesses of aerogel blankets were equal (10 mm), blanket A showed a better insulating performance decreasing heat loss than blankets B and C, respectively.

The calculated annual heat losses with different units are tabulated in Table 28, and the annual heat losses [kWh/year] are shown in Figure 42.

Table 28. The annual heat loss results for aerogel blankets.

	A (10 mm)	B (15 mm)	B (10 mm)	C (10 mm)	Bare pipe without insulation
Q_{loss} [W]	74.2	56.15	75.66	83.06	191.8
Q_a [kJ/year]	$2.340*10^6$	$1.771*10^6$	$2.386*10^6$	$2.619*10^6$	$6.049*10^6$
Q_{a2} [MJ/year]	2340	1171	2386	2619	6049
Q_{a3} [kWh/year]	650	491.9	662.8	727.6	1680
Q_{loss_10} for 10km long pipe [W]	267.6	283	290.4	262.7	$1.918*10^7$
Q_{a_10} [kJ/year]	$8.439*10^6$	$8.924*10^6$	$9.158*10^6$	$8.286*10^6$	$6.049*10^{10}$
Q_{a2_10} [MJ/year]	8439	8924	9158	8286	$6.049*10^7$
Q_{a3_10} [kWh/year]	2344	2479	2544	2302	$1.680*10^7$
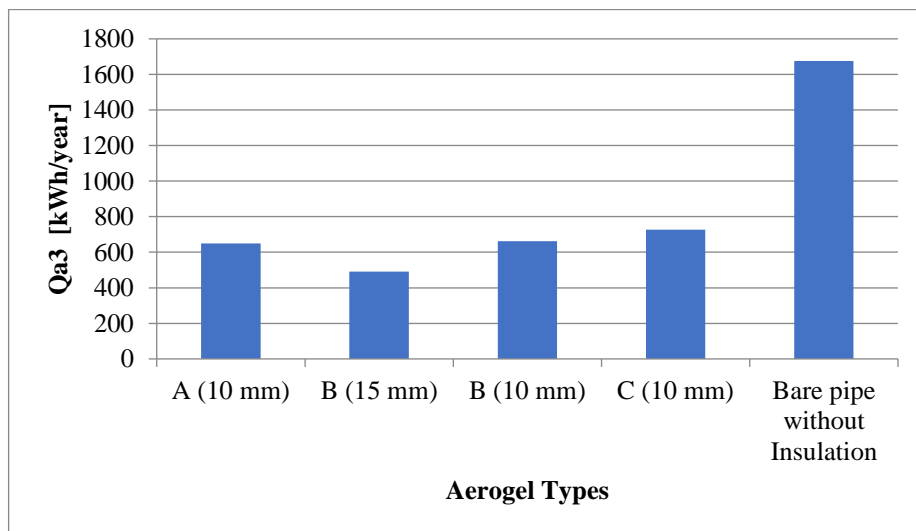
Figure 42. The comparison chart for annual heat losses with and without aerogel blankets.

As seen from Table 28 and Figure 42, aerogel insulation materials A (10 mm), B (15 mm), B (10mm) and, C (10 mm) decrease the heat loss by 61.3, 70.7, 60.6 and, 56.7% compared to the bare pipe, respectively. As the actual piping length is approximately 10 kilometers, assuming that the pipe diameter is constant and heat loss calculations for 10 kilometers were evaluated.

5.3.2. Rock wools

Thermal conductivity measurement results were used to determine the correct solutions for each rock wool sample. Since the rock wools and aerogel blankets have different thicknesses, two more cases are calculated for the rock wools, which are assumed to have the same thickness of 10 mm as the aerogel blankets. Another case was calculated without insulation material to make a complete comparison study. Calculated parameters for rock wool samples are listed in Table 29.

Table 29. Energy analysis results for rock wools.

	Old (100 mm)	New (100 mm)	Old (10 mm)	New (10 mm)	Bare pipe without insulation
k_{ins} [W/mK]	0.0393	0.0348	0.0393	0.0348	-
r_3 [m]	0.2365	0.2365	0.1465	0.1465	-
T_s [K]	302.5	300.2	369.3	369	379.1
h_i [W/m^{2}K]	1799	1799	1799	1799	1799
h_{conv} [W/m^{2}K]	0.0446	0.03621	0.08487	0.08484	0.08998
h_{rad} [W/m^{2}K]	5.824	5.756	8.071	8.059	5.306
h_o [W/m^{2}K]	5.868	5.792	8.155	8.144	5.396

Cont. of Table 29.

U [W/ m²K]	0.4271	0.3801	2.378	2.185	4.609
R_t [m²K/W]	2.341	2.631	0.4204	0.4577	0.217
q [W/m]	50.33	44.79	173.6	159.5	313.5

For three different cases;

- When the used and unused rock wool samples (100 mm) are compared, the new one shows lower heat loss through the unit pipe, about 12.4%.
- If rock wools have the same thickness as aerogel blankets (10 mm), the new rock wool shows better insulating properties than the used one, about 8.1%.
- The cold-drawn steel pipe without insulation loses the most heat.

This comparative study shows that the thickness of the insulation material plays a severe role in heat loss. And the estimated annual heat losses for rock wool samples are tabulated in Table 30 and shown in Figure 43.

Table 30. The annual heat loss results for rock wools.

	Old (100 mm)	New (100 mm)	Old (10 mm)	New (10 mm)	Bare pipe without insulation
Q_{loss} [W]	33.87	30.14	188.6	173.3	365.5
Q_a [kj/year]	$1.068*10^6$	950605	$5.948*10^6$	$5.464*10^6$	$1.153*10^7$
Q_{a2} [MJ/year]	1068	950.6	5948	5464	11526
Q_{a3} [kWh/year]	296.7	264.1	1652	1518	3202

Cont. of Table 30.

Q_{loss_10} for 10km long pipe [W]	686	677	592.1	591.2	3.655×10^6
Q_{a_10} [kJ/year]	2.163×10^7	2.135×10^7	1.867×10^7	1.865×10^7	1.153×10^{11}
Q_{a2_10} [MJ/year]	21634	21351	18672	18645	1.153×10^8
Q_{a3_10} [kWh/year]	6009	5931	5187	5179	3.202×10^7
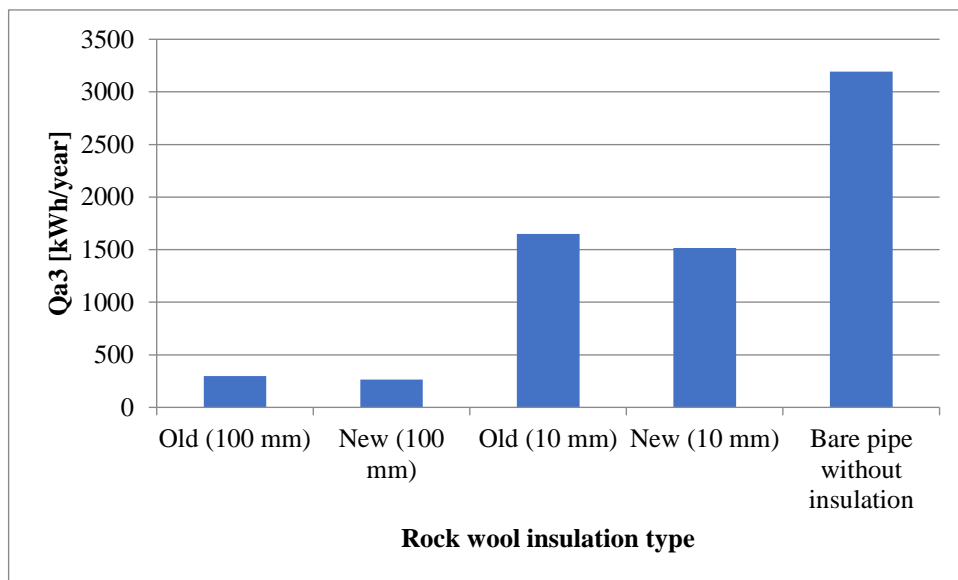
Figure 43. A bar chart for the annual heat losses with and without rock wool insulation.

As seen from Table 30 and Figure 43, old and new rock wool insulation materials with 100 mm of thickness decrease the heat loss in comparison with bare pipe by 90.7 and 91.7%; and by 48.4 and 52.6% with the thickness of 10 mm.

5.4. Summary of Results

A summary of the results chapter is made in this section. Table 31 is for the aerogel insulation blankets, and Table 32 is for the rock wool insulation material.

Table 31. Summary of aerogel blanket analyzes.

Temperature measurements	Measurement point	9	10	6	7	3	4
	Temperature (°C)	50.3	47.6	53.3	48.3	47.7	44.,2

	A	B	C
Thickness (mm)	10	15	10
Fiber diameters (μm)	10	14	10
Thermal conductivity coefficient (without cover) (W/mK)	0.0312	0.0278	0.0330
Thermal conductivity coefficient (with cover) (W/mK)	0.05	0.042	0.0433
Heat capacity (C_p) (J/gK)	1.16	1.36	1.50
Density (110°C) (kg/m^3)	162	178	191
Density (765°C) (kg/m^3)	156	170	184
Contact angle (blanket) (°)	146	100	125
Contact angle (cover) (°)	127	145	129
Heat loss (W)	74.2	56.15	83.06
The annual heat loss (kWh/year)	650	491.9	727.6

Table 32. Summary of rock wool analyzes.

		Old			New		
Temperature measurements	Measurement point	1	2	3	1'	2'	3'
	Temperature (°C)	27.7	30.0	30.3	27.9	26.4	25.5
Thickness (mm)		100					
Thermal conductivity coefficient (W/mK)		0.0393			0.0348		
Heat capacity (C_p) (J/gK)		1.73			1.69		
Density (110°C) (kg/m^3)		92.5			124.2		
Density (765°C) (kg/m^3)		89.2			121.9		
Contact angle (°)		134			147		
Heat loss (W)		33.87			30.14		
Heat loss – 10 mm (W)		188.6			173.3		
The annual heat loss (kWh/year)		296.7			264.1		
The annual heat loss - 10 mm (kWh/year)		1652			1518		

CHAPTER 6

CONCLUSIONS

Although the most critical parameters for the selection of insulation material are the thermal conductivity that is directly related to heat losses and contact angle (non-wetting), many analyses have been made regarding the micro-structure, considering that it is important to determine and interpret the microstructure of the materials, which can affect these parameters.

When the study is considered as a whole, it should be kept in mind that the measurements of both insulation materials (aerogel blanket and rock wool) were made at different times and conditions. At the same time, pipe diameters to which insulation materials are applied are also different.

Accordingly, all three aerogel blankets are composed of glass fiber with similar compositions and attached aerogels. The aerogel particles in the aerogel sample C are larger and adhere better to the fibers. This feature is valuable in terms of the continuity of the thermal insulation performance. When all the results are evaluated together, although the thermal conductivity of aerogel blanket C (without cover) is the highest, it gives the lowest surface temperature in field measurements. When the cover material is added, the thermal conductivities increase due to the higher thermal conductivity of the cover material. When aerogel blanket C is considered as blanket+cover, it is seen that it has a thermal conductivity close to aerogel blanket B. However, this still does not explain the lower surface temperature of aerogel blanket C.

There is no data on the change in thermal performance of the analysed aerogel blankets over time. However, when the blankets are touched, it is seen that the aerogel they contain is poured into powder form. The spillage of these powder aerogels, which improve the thermal performance of the blankets during use (preparing for assembly, hitting the surface, etc.), will adversely affect the thermal performance. Therefore, care should be taken during application and use. Microstructural analysis of all three samples showed higher adhesion in the sample of aerogel blanket C. Therefore, it is likely to measure lower surface temperature than aerogel blankets A and B. In addition, due to this

feature, it is thought that the performance loss of aerogel blanket C will be lower depending on time.

Another reason why the surface temperature of aerogel blanket C is lower is that its heat capacity is higher than other blankets. The large heat capacity slows down the heat transfer and is preferred for insulation purposes. Aerogel blanket B is 5 mm thicker than other felts. It can be a disadvantage in terms of cost and usage. So, the energy analysis was evaluated assuming that the aerogel blanket has the same thickness as other aerogel blankets.

Considering the non-wetting property, the sample with the highest contact angle is aerogel blanket A. Aerogel blanket A is followed by C and B. Since the cover material protects the aerogel blanket from the external environment, the contact angle measurement is more important than the blanket. The contact angle of cover material is in aerogel blankets B, C, and A from high to low. Since the contact angle is over 90° for all samples and covers, they are all suitable for use in geothermal application.

When the results are evaluated for rock wools, it is seen that the old rock wool is not entirely decomposed and is not wet. The fact that the contact angles of both rock wools are higher than 90°C reveals that they cannot be wetted in a short time. However, there is no value in how both rock wools may change with exposure to liquid over time.

It has been observed that rock wool can be shed as particles transporting, attaching, using, and disassembling from the production stage. Considering this situation and comparing the microscope images of rock wool, it is seen that the old rock wool is more porous. Increasing the porosity will decrease the density. The density- thermal conductivity relationship proves that the thermal conductivity decreases with the increase in the density expected to be seen in thermal insulation materials. Since the thermal insulation is expected to be inversely proportional to the heat transfer coefficient, the thermal performance of the new rock wool is better than the old rock wool.

As expected, the cold-drawn steel pipe without any insulation tends to have the highest heat loss in both pipes (DN150 and DN250). It should be noted that this research does not include estimations for optimum insulating thickness, but it has been observed that the insulation thickness has a direct effect on preventing heat losses. For the equal thicknesses in aerogel blankets, blanket A decreased the heat loss better than the blankets B and C, respectively. In rock wools, it was expected that the new-unused one tends to

show better properties than the old-used one, and in comparison with the bare pipe the new rock wool decreases heat loss more than the old rock wool. Rock wool reduces heat loss by 48-52% with a 10 mm thickness compared to bare pipe, and aerogel insulation blankets reduce heat loss by 57-61% with a 10 mm thickness compared to the bare pipe.

Considering the average dollar rate in Turkey of 14 TL in 2022, the price of aerogels is approximately 2100 TL/m^3. This value is about four times higher than the rock wool. In general, although the non-wetting feature of aerogel blankets is better, it will not be an economically acceptable choice for industrial use.

Suggestions for further study:

(1) Optimum thickness calculations of the insulation materials to be used in the Izmir Geothermal Energy Inc. can be done. The effect of pipe diameters on heat loss can be examined. In the same way, economic analysis can be done for the whole district heating piping system.

(2) As new aerogel synthesis researches are more focused on cellulosic aerogels for ecological purposes, a similar study can be conducted on synthesis, environmental effects, health aspects, economics and thermal performances of new cellulosic aerogels.

REFERENCES

[1]   Comakli K, Yuksel B, Bakirci K, Bölgesel Isıtma Sistemleri Boru Hatlarında Meydana Gelen Enerji ve Enerji Kayıpları. *Tesisat Mühendisliği Dergisi* **2006**, 91: 33- 38.

[2]   -TS 825 - mmo.org.tr https://www1.mmo.org.tr/resimler/dosya_ekler/cf3e258fbdf3eb7_ek.pdf (accessed Jan 13, 2022).

[3]   https://www.resmigazete.gov.tr/eskiler/2008/12/20081205-9.htm (accessed May 13, 2022).

[4]   Kaya S., Oguz M. E., Tesisat Yalitiminda Uygun Malzeme Seçimi. 12. *Ulusal Tesisat Mühendisligi Kongresi*, **2015**, 2483

[5]   Jóhannesson, T.; Guðmundsdóttir, V.; Einarsson, Ó. P.; Brauchler, R.; Lise, W.; Ince, C.; Vögeli, A. rep.; **2020**.

[6]   Izka.org.tr https://izka.org.tr/wp-content/uploads/2022/03/jeotermal.pdf (accessed May 11, 2022).

[7]   İzmir jeotermal Enerji san. ve tic. https://www.izmirjeotermal.com.tr/ (accessed Feb 17, 2020).

[8]   Thornbury, W. D. Mineral Wool Industry of the United States. *Economic Geography* **1938**, *14* (4), 398.

[9]   E. Brum Dutra da Rocha, A.M.F. de Sousa, Cristina.Russi.Guimarã. Furtado Properties Investigation of novel nitrile rubber composites with rockwool fibers, *Polymer Testing*, **2020**

[10]   Sanayi şiltesi https://www.izocam.com.tr/tr/urunler/sanayi-yalitimi/sanayi-siltesi (accessed Nov 26, 2021).

[11]   Hao, W.; Xu, J.; Li, R.; Zhao, X.; Qiu, L.; Yang, W. Developing Superhydrophobic Rock Wool for High-Viscosity Oil/Water Separation. *Chemical Engineering Journal* **2019**, *368*, 837–846.

[12]   Deutsch, D. http://suflux.com/EN/products/Supercritical_Dry_System.html (accessed May 10, 2020).

[13]   Hebalkar, N. Development of Nanoporous Aerogel-Based Thermal Insulation Products:'Make in India' Initiative. *Current Science* **2017**, *112* (07), 1413.

[14]   Aegerter, M. A.; Prassas, M. Aerogels Handbook. **2011**.

[15]   Hu, L.; He, R.; Lei, H.; Fang, D. Carbon Aerogel for Insulation Applications: A

Review. *International Journal of Thermophysics* **2019**, *40* (4).

[16] Kistler, S. S. Coherent Expanded Aerogels. *Rubber Chemistry and Technology* **1932**, *5* (4), 600–603.

[17] Pierre, A. C.; Pajonk, G. M. Chemistry of Aerogels and Their Applications. *Chemical Reviews* **2002**, *102* (11), 4243–4266.

[18] Soleimani Dorcheh, A.; Abbasi, M. H. Silica Aerogel; Synthesis, Properties and Characterization. *Journal of Materials Processing Technology* **2008**, *199* (1-3), 10–26.

[19] Dervin, S.; Pillai, S. C. An Introduction to Sol-Gel Processing for Aerogels. *Advances in Sol-Gel Derived Materials and Technologies* **2017**, 1–22.

[20] Gurav, J. L.; Jung, I.-K.; Park, H.-H.; Kang, E. S.; Nadargi, D. Y. Silica Aerogel: Synthesis and Applications. *Journal of Nanomaterials* **2010**, *2010*, 1–11.

[21] Pajonk, G. M.; Repellin-Lacroix, M.; Abouarnadasse, S.; Chaouki, J.; Klavana, D. From Sol-Gel to Aerogels and Cryogels. *Journal of Non-Crystalline Solids* **1990**, *121* (1-3), 66–67.

[22] Koebel, M.; Rigacci, A.; Achard, P. Aerogel-Based Thermal Superinsulation: An Overview. *Journal of Sol-Gel Science and Technology* **2012**, *63* (3), 315–339.

[23] Prevolnik, V.; Kraner Zrim, P.; Rijavec, T. Textile Technological Properties of Laminated Silica Aerogel Blanket. *Contemporary Materials* **2014**, *5* (1).

[24] Lakatos, Á.; Trnik, A. Thermal Characterization of Fibrous Aerogel Blanket. *MATEC Web of Conferences* **2019**, *282*, 01001.

[25] Stepanian, C. J. Highly Flexible Aerogel Insulated Textile-like Blankets, US Patent Application Publication.

[26] Umberto, B.; (Mark) Zaidi, S. Characterization of Commercial Aerogel-Enhanced Blankets Obtained with Supercritical Drying and of a New Ambient Pressure Drying Blanket. *Energy and Buildings* **2019**, *198*, 542–552.

[27] HARRISON, R.; MORTIMER, N. D.; SMARASON, O. B. Geothermal District Heating in Iceland. *Geothermal Heating* **1990**, 468–541.

[28] About geothermal district heating http://geodh.eu/about-geothermal-district-heating/ (accessed Jun 14, 2020).

[29] Keçebaş, A.; Ali Alkan, M.; Bayhan, M. Thermo-Economic Analysis of Pipe Insulation for District Heating Piping Systems. *Applied Thermal Engineering* **2011**, *31* (17-18), 3929–3937.

[30] BAKER, D. K.; SHERIF, S. A. Heat Transfer Optimization of a District Heating System Using Search Methods. *International Journal of Energy Research* **1997**, *21* (3), 233–252.

[31] Böhm, B. On Transient Heat Losses from Buried District Heating Pipes. *International Journal of Energy Research* **2000**, *24* (15), 1311–1334.

[32] Adamo, L.; Cammarata, G.; Fichera, A.; Marletta, L. Improvement of a District Heating Network through Thermoeconomic Approach. *Renewable Energy* **1997**, *10* (2-3), 213–216.

[33] Gustafsson, S.-I. Optimisation of Insulation Measures on Existing Buildings. *Energy and Buildings* **2000**, *33* (1), 49–55.

[34] Stojanovic , A.; Koebel, M. Low Cost Silica Aerogel Production. **2015**.

[35] Jensen, K. I., Kristiansen, F. H., & Schultz, J. M., Highly Insulating and Light Transmitting Aerogel Glazing for Super Insulating Windows (HILIT+): – *publishable final technical report*, **2005** EU-FP5 contract ENK6-CT-2002-00648.

[36] Nocentini, K.; Achard, P.; Biwole, P.; Stipetic, M. Hygro-Thermal Properties of Silica Aerogel Blankets Dried Using Microwave Heating for Building Thermal Insulation. *Energy and Buildings* **2018**, *158*, 14–22.

[37] Dr. Owen Evans. Aerogel-Based Insulation for High-Temperature Industrial Processes. **2011**.

[38] Yu, H.; Liang, X.; Wang, J.; Wang, M.; Yang, S. Preparation and Characterization of Hydrophobic Silica Aerogel Sphere Products by Co-Precursor Method. *Solid State Sciences* **2015**, *48*, 155–162.

[39] Fantucci, S.; Fenoglio, E.; Serra, V.; Perino, M.; Dutto, M.; Marino, V. Hygrothermal Characterization of High-Performance Aerogel-Based Internal Plaster. *Sustainability in Energy and Buildings* **2019**, 259–268.

[40] Siligardi, C.; Miselli, P.; Francia, E.; Lassinantti Gualtieri, M. Temperature-Induced Microstructural Changes of Fiber-Reinforced Silica Aerogel (FRAB) and Rock Wool Thermal Insulation Materials: A Comparative Study. *Energy and Buildings* **2017**, *138*, 80–87.

[41] Chakraborty, S.; Pisal, A. A.; Kothari, V. K.; Venkateswara Rao, A. Synthesis and Characterization of Fibre Reinforced Silica Aerogel Blankets for Thermal Protection. *Advances in Materials Science and Engineering* **2016**, *2016*, 1–8.

[42] Hoseini, A.; McCague, C.; Andisheh-Tadbir, M.; Bahrami, M. Aerogel Blankets: From Mathematical Modeling to Material Characterization and Experimental Analysis. *International Journal of Heat and Mass Transfer* **2016**, *93*, 1124–1131.

[43] testo 925 https://www.testo.com/en-TH/testo-925/p/0560-9250 (accessed May 24, 2022).

[44] Yuan, Y.; Lee, T. R. Contact Angle and Wetting Properties. *Surface Science Techniques* **2013**, 3–34.

[45] Zong, S.; Wei, W.; Jiang, Z.; Yan, Z.; Zhu, J.; Xie, J. Characterization and Comparison of Uniform Hydrophilic/Hydrophobic Transparent Silica Aerogel Beads: Skeleton Strength and Surface Modification. *RSC Advances* **2015**, *5* (68), 55579–55587.

[46] Keçebaş A., Determination of Optimum Insulation Thickness for Energy Saving thought Pipe Insulation in District Heating Systems. *Electronic Journal of Machine Technologies*, **2012,** *9(1)* 1-14

[47] Resources, e-M. Chart software : Engineering software https://fchartsoftware.com/ees/ (accessed Feb 17, 2022).

[48] BERGMAN, THEODOREL. *Fundamentals of Heat and Mass Transfer*, 6th ed.; WILEY: S.l., 2006.

[49] Shafi, S., & Zhao, Y., Superhydrophobic, enhanced strength and thermal insulation silica aerogel/glass fiber felt based on methyltrimethoxysilane precursor and silica gel impregnation. *Journal of Porous Materials*, **2019**, *27*(2), 495–502.

[50] Izocam Glasswool https://www.izocam.com.tr/pdffiles/msdspdf/MSDS%20GW_EN128.pdf (accessed Nov 10, 2021).

[51] Izocam Glasswool https://www.izocam.com.tr/pdffiles/msdspdf/%C4%B0ZOCAM_GW_MSDS_EN 557.pdf (accessed Nov 10, 2021).